BMC
Plant Biology

RESEARCH ARTICLE   **Open Access**

The response and recovery of the *Arabidopsis thaliana* transcriptome to phosphate starvation

Jongchan Woo[1†], Cameron Ross MacPherson[1,4†], Jun Liu[1], Huan Wang[1,3], Takatoshi Kiba[1], Matthew A Hannah[2], Xiu-Jie Wang[3], Vladimir B Bajic[4] and Nam-Hai Chua[1*]

Abstract

Background: Over application of phosphate fertilizers in modern agriculture contaminates waterways and disrupts natural ecosystems. Nevertheless, this is a common practice among farmers, especially in developing countries as abundant fertilizers are believed to boost crop yields. The study of plant phosphate metabolism and its underlying genetic pathways is key to discovering methods of efficient fertilizer usage. The work presented here describes a genome-wide resource on the molecular dynamics underpinning the response and recovery in roots and shoots of *Arabidopsis thaliana* to phosphate-starvation.

Results: Genome-wide profiling by micro- and tiling-arrays (accessible from GEO: GSE34004) revealed minimal overlap between root and shoot transcriptomes suggesting two independent phosphate-starvation regulons. Novel gene expression patterns were detected for over 1000 candidates and were classified as either initial, persistent, or latent responders. Comparative analysis to AtGenExpress identified cohorts of genes co-regulated across multiple stimuli. The hormone ABA displayed a dominant role in regulating many phosphate-responsive candidates. Analysis of co-regulation enabled the determination of specific versus generic members of closely related gene families with respect to phosphate-starvation. Thus, among others, we showed that *PHR1*-regulated members of closely related phosphate-responsive families (*PHT1;1*, *PHT1;7–9*, *SPX1-3*, and *PHO1;H1*) display greater specificity to phosphate-starvation than their more generic counterparts.

Conclusion: Our results uncover much larger, staged responses to phosphate-starvation than previously described. To our knowledge, this work describes the most complete genome-wide data on plant nutrient stress to-date.

Keywords: Phosphate starvation, Response and recovery, Roots and shoots, Organ specific, Whole seedling, Initial, Persistent, and Latent expression patterns, Functional analysis, Comparative analysis with AtGenExpress, Micro-array and tiling-array, Hydroponic culture

Background

Phosphorus is one of the most important macronutrients in crop fertilizers [1,2]. Although it is required in only small quantities [3] most crop plants require inorganic forms of phosphorous such as phosphate (P_i) that is not readily available in many soil conditions [4,5]. Because of P_i-limiting stress, P_i fertilizers are used in agriculture to elevate soil P_i concentrations to increase crop productivity [4]. However, over-application of P_i fertilizers has led to

run-off of excess P_i into waterways damaging ecosystems [6-8]. Therefore, there is economic and ecological impetus underlying research into plant P_i signaling pathways with the expectation that results from such work may help to develop crop plants with enhanced P_i use efficiency, thereby mitigating the unwarranted, excessive application of P_i fertilizers.

Whereas many researchers have studied P_i signaling in the model plant *Arabidopsis thaliana*, it is only recently that high-throughput technologies have been applied to address this issue [9-14]. To date, a limited amount of genome-wide data is available and there is no one dataset that can serve as a reference for comparison in studies on P_i-signaling. Our ability to relate one genome-wide study to

* Correspondence: chua@mail.rockefeller.edu
†Equal contributors
[1]Laboratory of Plant and Molecular Biology, The Rockefeller University, New York 10065, NY, USA
Full list of author information is available at the end of the article

another is, therefore, constrained by insufficient data. Here, we aimed to construct a referable dataset by recording and characterizing the response and recovery of *Arabidopsis thaliana*'s whole genome transcriptome to P_i starvation (P_i^{starv}) at a higher resolution than previously reported.

Previous studies have implicated common sets of differentially regulated genes during related P_i^{starv} treatments but a large degree of variation exists among independent studies (see Additional file 1). Several factors may contribute to this observed variation: (1) Different methodologies were used to manipulate P_i concentrations in the local environment; (2) Different tissues, organs, and plant species were studied, that may implement different P_i-sensing and gene response circuitry; (3) Previous work did not analyze independent responses of roots and shoots on a genome-wide scale; (4) Due to natural P_i-reservoirs in plant samples it is difficult to determine the duration of starvation treatment; (5) There is a lack of a comprehensive study serving as a basic reference.

To address the above-mentioned issues we aimed to not only identify novel genetic components in the Arabidopsis P_i^{starv} response but also provide results that can serve as a reference for future investigations. To this end, we designed experiments to evaluate differential gene expression separately in roots and shoots of plants subjected to P_i^{starv} ("response" phase) followed by return to replete conditions ("recovery" phase). In total, we analyzed 18 micro- and 18 tiling-arrays consisting of the following sample structure: 3 biological replicates sampled from 2 organs (roots and shoots), each exposed to 3 conditions (mock (P_i^{mock}), starvation (P_i^{starv}), and replete ($P_i^{replete}$)). Gene response was evaluated by contrasting P_i^{starv} against P_i^{mock}, whereas gene recovery was calculated by contrasting $P_i^{replete}$ versus P_i^{starv} samples. In this way, we aimed to address the first three issues by providing a common reference for the analysis of organ-specific response and recovery. To address (4) we provided molecular evidence to demonstrate that genes did indeed respond to, and subsequently recovered from, P_i^{starv}. We addressed (5), in part, as our experimental model generated a high-quality dataset by analyzing both response-and-recovery data from plants conditioned in the same environment using both the ATH1 micro-array and the tiling-array platform for transcriptome analysis.

Our data indicated a dramatic difference in the molecular responses of roots and of shoots both during and post P_i^{starv}. We showed that significantly different regulons are involved in P_i^{starv} in both a time and organ dependent manner. Furthermore, in comparative studies with micro-array data generated by the AtGenExpress initiative we developed a method for the determination of specific versus generic members of closely related gene families with respect to P_i^{starv}.

Being a genome-wide study, we identified many genes previously unknown to respond to and/or recover from P_i^{starv}. To further verify the specificity of their functions we conducted literature surveys on possible co-regulation by other stresses of many candidates. We believe that our work collectively describes the highest resolution of genome-wide data available to the community to date. The accession code, GSE34004, may be used to access the micro- and tiling-array data from the Gene Expression Omnibus (GEO).

Results
Experimental design and quality assessment
We incorporated organ specific P_i^{starv} treatment and recovery into one set of experiments. Briefly, we grew seedlings in P_i sufficient media for 20 days, followed by 10 days in P_i deficient (P_i^{starv}) or sufficient (P_i^{mock}) media to measure gene expression response. Plants grown in P_i deficient media were then transferred to P_i sufficient media for an additional 3 days ($P_i^{replete}$) for recovery. Roots and shoots were separately collected from various plant samples in 3 replicate experiments. By considering three treatments (P_i^{mock}, P_i^{starv}, and $P_i^{replete}$) we uncovered genes with basal expression during response and recovery, genes that initially responded to P_i^{starv}, genes that persisted (did not recover) in their initial response during recovery and genes that latently responded during the recovery phase only. These 4 states allowed us to define 9 classes of gene expression patterns (Table 1), and by comparing root and shoot responses, we were able to observe up to 81 (9^{root}x9^{shoot}) classes describing organ-specific or -common gene expression patterns (Figure 1i).

To increase confidence in the observed changes, we used two independent platforms to detect genome-wide expression changes. We first hybridized all cDNA samples to Affymetrix ATH1 micro-arrays. After having determined each chip to be of sufficient quality we continued to detect differentially regulated genes during response (P_i^{starv}/P_i^{mock}) and recovery ($P_i^{replete}$/P_i^{starv}) (see Additional file 2). Subsequently, we used principal component analysis (PCA) to analyze the orthogonal relationship between gene response and recovery, and between roots and shoots (Figure 2a,b). Indeed, where the 1st PC likely accounted for broad variations, the 2nd and 3rd PCs captured true biological phenomena. For example, the 2nd PC accounted for 12% of the total variation (Figure 2a) and clearly distinguished between root and shoot samples (Figure 2b-xAxis); and, the 3rd PC highlighted differences between P_i^{mock}, P_i^{starv}, and $P_i^{replete}$ treatments (Figure 2b-yAxis). Significantly, according to the 3rd PC, P_i^{mock} and $P_i^{replete}$ treatments were closely related in both roots and shoots indicating recovery from P_i^{starv} in both organs.
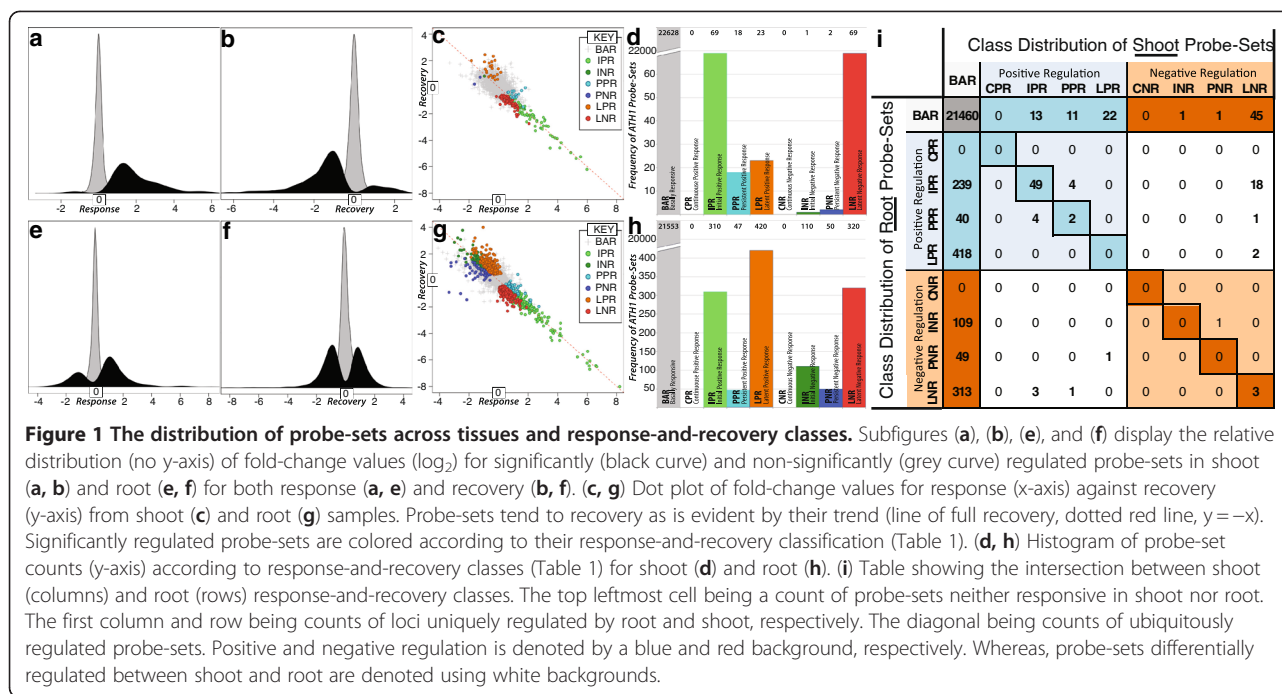
Table 1 Response-and-recovery classification scheme for loci

Class	Code	Response		Recovery		Cartoon representation
		p-Value*	log$_2$(FC)	p-Value*	log$_2$(FC)	
Basal **R**esponse	**BAR**	*no change*		*no change*		
Continuous **P**ositive **R**esponse	**CPR**	≤ 0.001	+	≤ 0.001	+	
Initial **P**ositive **R**esponse	**IPR**	≤ 0.001	+	≤ 0.001	-	
Persistent **P**ositive **R**esponse	**PPR**	≤ 0.001	+	*no change*		
Latent **P**ositive **R**esponse	**LPR**	*no change*		≤ 0.001	+	
Continuous **N**egative **R**esponse	**CNR**	≤ 0.001	-	≤ 0.001	-	
Initial **N**egative **R**esponse	**INR**	≤ 0.001	-	≤ 0.001	+	
Persistent **N**egative **R**esponse	**PNR**	≤ 0.001	-	*no change*		
Latent **N**egative **R**esponse	**LNR**	*no change*		≤ 0.001	-	

By table headings: (Class) All loci are binned into 1 of 9 response-and-recovery classes; (Code) Classes are given a 3 letter code for convenience. (Response) The *p-value* and log$_2$ fold-change required by a locus' response in order to qualify for the respective class. (Recovery) The *p-value* and log$_2$ fold-change required by a locus' recovery in order to qualify for the respective class. A "*no change*" is indicated if the *p-value* is not less than or equal to 0.001. (Cartoon Representation) A cartoon diagram indicating the general expression pattern captured by the class.

To increase confidence in our data we hybridized identical cDNA libraries to Affymetrix tiling-arrays 1.0R, which were processed using cisgenome software [15]. We initially evaluated data parity between the two platforms by calculating correlation of fold-change between probe-sets present on the ATH1 arrays and their corresponding probes on the tiling-arrays 1.0R. The correlation between the two platforms was above 0.8 for the root-response, root-recovery, leaf-response and leaf-recovery (Figure 2c). In addition, we confirmed transcript levels of

Class Distribution of Shoot Probe-Sets

	BAR	Positive Regulation				Negative Regulation			
		CPR	IPR	PPR	LPR	CNR	INR	PNR	LNR
BAR	21460	0	13	11	22	0	1	1	45
CPR	0	0	0	0	0	0	0	0	0
IPR	239	0	49	4	0	0	0	0	18
PPR	40	0	4	2	0	0	0	0	1
LPR	418	0	0	0	2	0	0	0	2
CNR	0	0	0	0	0	0	0	0	0
INR	109	0	0	0	0	0	0	1	0
PNR	49	0	0	0	1	0	0	0	0
LNR	313	0	3	1	0	0	0	0	3

(Left axis: Class Distribution of Root Probe-Sets — Positive Regulation: CPR, IPR, PPR, LPR; Negative Regulation: CNR, INR, PNR, LNR)

Figure 1 The distribution of probe-sets across tissues and response-and-recovery classes. Subfigures (**a**), (**b**), (**e**), and (**f**) display the relative distribution (no y-axis) of fold-change values ($\log_2$) for significantly (black curve) and non-significantly (grey curve) regulated probe-sets in shoot (**a, b**) and root (**e, f**) for both response (**a, e**) and recovery (**b, f**). (**c, g**) Dot plot of fold-change values for response (x-axis) against recovery (y-axis) from shoot (**c**) and root (**g**) samples. Probe-sets tend to recovery as is evident by their trend (line of full recovery, dotted red line, $y = -x$). Significantly regulated probe-sets are colored according to their response-and-recovery classification (Table 1). (**d, h**) Histogram of probe-set counts (y-axis) according to response-and-recovery classes (Table 1) for shoot (**d**) and root (**h**). (**i**) Table showing the intersection between shoot (columns) and root (rows) response-and-recovery classes. The top leftmost cell being a count of probe-sets neither responsive in shoot nor root. The first column and row being counts of loci uniquely regulated by root and shoot, respectively. The diagonal being counts of ubiquitously regulated probe-sets. Positive and negative regulation is denoted by a blue and red background, respectively. Whereas, probe-sets differentially regulated between shoot and root are denoted using white backgrounds.

37 genes selected from both platforms by quantitative reverse transcriptase PCR (qRT-PCR, see Additional file 3).
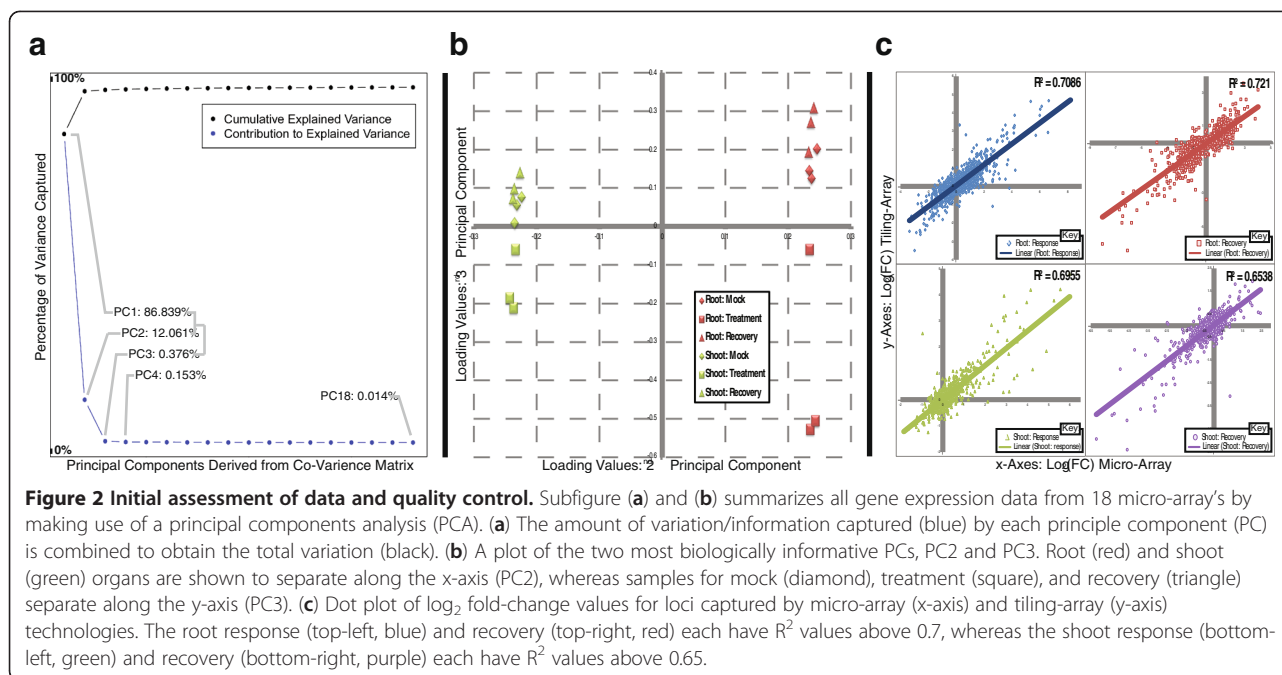
Novel P_i-signaling patterns observed among genes involved in P_i^{starv}

Response-and-recovery gene expression patterns in roots and shoots

Arabidopsis roots displayed several novel responses to P_i^{starv} not observed in previous genome-wide studies. Several previous studies have each independently identified gene sets that initially respond to [9,11,12] or recover from P_i^{starv} [10]. However, we were able to additionally identify genes that persisted in their expression during the 3-day recovery period and others that latently responded to P_i^{starv} during recovery. Moreover, we were able to characterize these responses in an organ-specific manner. A total of 1,257 genes detected by ATH1 probe-sets (henceforth referred to as gene/s) were differentially expressed in roots during either starvation or recovery. Table 1 highlights the criteria used to subclassify each of the 1,257 genes. A large proportion of root-responsive genes (310, ≈25%) fell into the "Initial Positive Response" class IPR. These genes were significantly up-regulated during starvation but returned to basal levels after recovery (Figure 1e,f,g,h). One hundred and ten genes (≈8%) were negatively regulated, falling into the "Initial Negative Response" class (INR). By contrast, 47 and 50 genes continued to be up- ("Persistent Positive Response", PPR) or down-regulated ("Persistent Negative Response", PNR), respectively, during recovery.

A significant proportion of the genes (58%) responded to recovery only after an initial priming by P_i^{starv}. We classified these latent genes into either the "Latent Positive Response" (LPR; 420 genes) or "Latent Negative Response" (LNR; 320 genes) class. Thus, the latent response of 740 genes (LPR + LNR) was of equal relevance to P_i-signaling as genes of the initial and persistent starvation responses combined (517 genes from IPR, INR, PPR, and PNR). However, as observed in Figure 1g, latently responsive genes (red/orange) are generally regulated to a lesser extent (fold-change) than initially responsive genes (dark-green/light-green).

For shoots, using the same criteria to identify differentially expressed genes as in roots (Table 1), we classified 182 genes into response-and-recovery classes (Figure 1a, b,c,d). Of these 182 genes, 69 (≈38%) were classified as IPR whereas only 1 was determined to be INR. Briefly, we classified the remaining 112 genes as follows: 18 PPR and 2 PNR; and, 23 LPR and 69 LNR. Other than the large LPR response in roots (Figure 1h), the distribution of gene numbers between root and shoot classes were similar, with the number of latently responsive genes (92 genes) approximately equal to those of the initial and persistent responses combined (90 genes). In addition, we noted that shoot tissues initially up-regulated 48% of all responsive genes and the remainder were latently down-regulated in shoots. Hence, shoot tissues show a distinct shift in gene expression patterns, from an almost absolute initial positive response to a similarly strong latent negative response.

Figure 2 Initial assessment of data and quality control. Subfigure (**a**) and (**b**) summarizes all gene expression data from 18 micro-array's by making use of a principal components analysis (PCA). (**a**) The amount of variation/information captured (blue) by each principle component (PC) is combined to obtain the total variation (black). (**b**) A plot of the two most biologically informative PCs, PC2 and PC3. Root (red) and shoot (green) organs are shown to separate along the x-axis (PC2), whereas samples for mock (diamond), treatment (square), and recovery (triangle) separate along the y-axis (PC3). (**c**) Dot plot of $\log_2$ fold-change values for loci captured by micro-array (x-axis) and tiling-array (y-axis) technologies. The root response (top-left, blue) and recovery (top-right, red) each have R^2 values above 0.7, whereas the shoot response (bottom-left, green) and recovery (bottom-right, purple) each have R^2 values above 0.65.

Gene expression in roots and shoots recover from P_i^{starv} after 3 days in replete conditions

Most of the significantly expressed genes, during the initial shoot (Figure 1a-black) and root (Figure 1e-black) responses, returned to basal expression levels after a 3 day recovery in P_i-sufficient conditions ($P_i^{replete}$). This is indicated by the general trend that genes had to spread across the $y = -x$ axis (Figure 1c,g – dashed red line), i.e. the axis of full-recovery. We note that of the 9 response-and-recovery classes, 2 were neither observed in shoots nor roots. These two undetected classes, "Continuous Positive Response" (CPR) and "Continuous Negative Response" (CNR) described genes that responded significantly and in the same manner during both response-and-recovery phases (Table 1). The absence of these classes in our dataset, together with the general trend of our data and the expression profile of P_i-starvation responsive non-coding RNAs *IPS1*, *miR399*, and *miR827* (see Additional file 4), confirmed that a 3-day period in P_i sufficient media was a suitable choice for the recovery period.

Co-expression versus organ specific gene expression patterns

Both roots and shoots responded to P_i^{starv} to varying degrees by differentially regulating initial and persistently responsive genes. P_i-signaling cascades were initiated in anticipation of $P_i^{replete}$ conditions, as observed by genes in the latently responsive class. The root response included 89 genes that were also differentially regulated among a total of 182 shoot responsive genes (Figure 1i-all rows and columns except the first). Yet, both organs displayed characteristic gene expression patterns. Furthermore, roots

accounted for 87% of the combined P_i-responsive genes in both organs. Consideration of the root/shoot response without the 89 ubiquitously regulated genes uncovered at least 2 tissue-specific and P_i-sensitive regulons. The 89 co-regulated genes may be involved in systemic P_i-signaling as 60% of these putative systemic-regulators were differentially regulated in the same manner in both organs (Figure 1i-diagonal). Thibaud et al. (2010) identified 42 systemically regulated genes of which 16 where basally regulated and 14 were considered to be regulated in both our root and shoot datasets. Of the remaining 35 genes in our study (40%), 8 and 1 were generally up- and down-regulated in roots and shoots, respectively; whereas, 26 genes displayed antagonistic behavior between the two organs.

The classification of response-and-recovery into 9 distinct classes reflected the molecular diversity in P_i-signaling during P_i^{starv}. The independent analysis of roots and shoots has aided in the identification of systemic versus organ-specific responses. Differential regulation of systemic and organ-specific genes is indicative of function related to the P_i^{starv} response. In the following, we present correlations between observed classes and annotations among public databases and current literature.

The response and recovery of genes absent from the micro-array platform

A clear advantage of the 1.0R tiling-array platform over the ATH1 micro-array is the detection of transcripts derived from genomic regions not covered by the micro-array's optimized probes. Indeed, TAIR8 has annotations for 26,956 nuclear protein-coding genes (AGI identifiers, PUBMedID: 22140109). Of these, 21,912 (81%) genes are

represented by probes on the ATH1 micro-array. With this in mind we set out to characterize the transcriptional response and recovery to P_i^{starv} of the remaining 5,044 genes undetectable by the ATH1 micro-array.

All genes with less than 3 representative probes on the 1.0R tiling-array were excluded from further analysis. For the remaining 4,730 genes, the transcript abundance for each treatment-condition was calculated using the same median-polish methodology as used in the micro-array analysis (PUBMedID: 18348734). The response of all genes (G_{1-n}) in roots was assessed by normalizing according to the standard deviation (σ) and declaring a gene as differentially expressed if $|G_i/\sigma| >= 3$. This ensured that only the most differentially expressed genes (top 1.5% in the root response) were considered to be regulated. This method was further employed to detect differential expression during root recovery, and again for the shoot response and recovery. Using this data, genes that are absent from the micro-array were classified into 1 of 9 response-and-recovery classes in a manner analogous to the classification of genes described by table 1. This method classified 477 out of the 4,730 tiling-array-specific genes as differentially expressed (Table 2); 171 genes were root specific, 242 were shoot specific, and 64 were systemically regulated. Details on the response and recovery for all 4,730 genes can be found in supplemental data (see Additional file 5).

Analysis of functionally related gene loci

Using GO-SLIM, we collected annotations and calculated *p-values* for all genes classified in both root and shoot datasets (1350 genes). The highest ranked term was, "cellular response to phosphate starvation" (Bonferroni adjusted *p-value* = 3.81×10^{-13}). Thirteen of the 21 genes annotated by this term were identified in genes expressed in both organs and they predominantly exhibited an IPR pattern. Several additional terms such as "galactolipid biosynthetic process" and "sugar:hydrogen symporter activity" were identified as significant. As expected, these terms described genes already known to be P_i responsive. Therefore, we aimed to extend current knowledge by focusing on gene expression changes in the context of response-and-recovery and in the two separate organs.

Expression patterns of known P_i responsive gene loci in roots and shoots

To facilitate comparison to prior studies, we were able to identify a total of 84 genes (AGI identifiers) that have been variously described in the literature and annotated by TAIR as being P_i-responsive (see Additional file 6). We clustered these 84 genes by their functional annotations (Figure 3-heatmap) and identified 8 partially overlapping functional clusters. Figure 3a-h shows the gene expression patterns for these known P_i-responsive genes

during both starvation and recovery in our root dataset. Generally, these 8 clusters grouped genes involved in transcription, plastid metabolism, response to wounding, P_i-transport, anthocyanin biosynthesis, and galacto- and glyco-lipid biosynthesis. Using a Bonferroni corrected *p-value* threshold of 0.001 we classified 30% of the 84 genes as IPR in roots. However, the majority (60%) of the known loci did not significantly respond. This is perhaps not surprising because these genes were aggregated from the results of many studies, each employing a distinct protocol. Of the remaining 10%, *PEPCK2* displayed a persistent positive response to starvation whereas *AAT* a persistent negative response. Two separate sets of genes each responded in roots in a latent manner: LPR (*PAP1, CAT3, PHO1*) and LNR (*UGP, ORF02, ATPPC1, LPR1*). Similar results were obtained when we performed the same analysis on gene expression levels in shoots. Comparison of the two organs showed that 14 genes (*ATPAP1, ATPAP17, PHT1;4, PHT1;7, PHO1;H1, PHF1, PLDP2, MGD2, MGD3, SQD1, SQD2, SPX1, SPX2, and SPX3*) shared IPR patterns among both. By contrast, the majority of the remaining IPR genes (*At3g03530, DGD2, PAP6, PHT1;3, PHT1;1, PHT1;8, PHT1;9, PHT1;5*) were non-responsive in shoots.

For the following functional analyses, gene lists were converted from lists of Affymetrix probe-ids to AGI identifiers. This step was necessary to maintain the accuracy of results, as the relationship between probe-ids and AGI identifiers is many-to-many, but probe-ids to transcript abundance and AGI-ids to functional-terms are one-to-one relationships.

In contrast to the 84 known P_i-responsive loci described above, we uncovered a more complex network of 1231 AGI gene identifiers that were also involved in root P_i^{starv}. Among these putative P_i-responsive genes we distinguished between those involved in the initial response from those in the latent response to P_i^{starv}. Upon further examination, we found that a small subset of 93 genes were neither aptly described as initial nor latent in their response patterns. Instead, these genes persisted in their initial expression and did not return to basal levels after a 3-day recovery; this was likely due to an insufficient recovery period for this group of genes. Thus, we investigated gene expression and function of these novel root P_i-responsive loci among 3 phases: 'INITIAL,' 'PERSISTENT,' and 'LATENT' (see Additional file 7).

Three gene expression phases uncover functional responses to P_i^{starv}

Considering both the response to and recovery from P_i^{starv}, we classified a gene's expression profile into one of three phases – initial, persistent, and latent. By definition, for a gene to be classified it had to be significantly differentially expressed in either the response to and/or recovery from

Table 2 Responsive and recovering genes absent from the ATH1 micro-array

Identifiers		Root			Shoot		
AGI	Symbol	Res.*	Rec.*	Class	Res.*	Rec.*	Class
			Systemically Regulated				
AT4G01060	CPL3/ETC3	4.291	−3.748	IPR	1.476	−1.505	IPR
AT5G43300	GDPD3	4.272	−4.045	IPR	2.121	−1.893	IPR
AT3G09922	IPS1	5.971	−4.591	IPR	6.572	−5.800	IPR
AT4G19038	LCR15	1.376	−2.223	LNR	1.143	−1.756	LNR
AT3G61172	LCR8	0.412	−1.981	LNR	0.518	−1.667	LNR
AT2G41240	BHLH100	−2.631	1.024	PNR	−3.980	1.716	INR
AT3G07005	LCR43	−1.692	0.274	PNR	1.687	−0.321	PPR
AT1G73607	LCR65	−2.178	−0.235	PNR	1.417	−1.490	IPR
AT3G56970	ORG2	−1.625	0.454	PNR	−4.283	1.894	INR
AT3G61177	LCR53	1.963	−1.140	PPR	−1.302	0.300	PNR
			Root Specific				
AT1G73165	CLE1	−1.977	1.924	INR	−0.107	−0.097	BAR
AT2G31081	CLE4	−2.012	2.875	INR	1.168	−0.746	BAR
AT2G31082	CLE7	−1.952	2.312	INR	0.111	0.121	BAR
AT5G24920	GDU5	−2.877	3.590	INR	0.217	0.223	BAR
AT3G06985	LCR44	−1.885	2.264	INR	1.002	−0.650	BAR
AT3G49570	LSU3	−2.308	1.684	INR	0.613	0.096	BAR
AT4G18197	PUP7	−1.770	1.755	INR	0.544	−0.300	BAR
AT1G54760	AGL85	1.941	−2.146	IPR	−0.136	−0.280	BAR
AT5G06905	CYP712A2	2.089	−2.979	IPR	−0.110	−0.599	BAR
AT3G30725	GDU6	3.627	−5.125	IPR	−0.030	−0.020	BAR
AT2G32960	PFA-DSP2	1.810	−1.706	IPR	1.185	−1.223	BAR
AT3G09400	PLL3	2.523	−2.929	IPR	0.978	−0.054	BAR
AT4G27920	RCAR4	2.259	−2.132	IPR	0.734	−0.431	BAR
AT1G53130	GRI	−0.375	−1.756	LNR	−0.056	−0.117	BAR
AT3G61182	LCR54	0.226	−1.759	LNR	−0.763	−0.202	BAR
AT2G14365	LCR84	0.519	−1.936	LNR	0.756	−0.101	BAR
AT4G10115	SCRL20	0.348	−2.985	LNR	−0.297	−0.485	BAR
AT4G29305	LCR25	−1.368	2.295	LPR	0.973	−0.521	BAR
AT4G06746	RAP2.9	−1.617	3.125	LPR	−0.404	0.512	BAR
AT4G23170	EP1	−2.487	0.662	PNR	−0.033	−0.134	BAR
AT4G09795	LCR13	−2.395	1.119	PNR	−0.939	0.103	BAR
AT3G23167	LCR39	−1.694	0.502	PNR	0.556	−1.297	BAR
AT4G18195	PUP8	−1.820	1.335	PNR	−0.136	−0.001	BAR
AT3G23715	SCRL13	−2.088	0.971	PNR	1.289	0.501	BAR
AT2G20825	ULT2	−1.640	0.337	PNR	0.339	0.139	BAR
AT5G45105	ZIP8	−2.392	0.846	PNR	0.284	−1.101	BAR
AT4G22210	LCR85	1.664	0.028	PPR	0.399	−0.238	BAR
AT1G60815	RALFL7	1.728	−0.550	PPR	0.315	0.319	BAR
			Shoot Specific				
AT1G47510	AT5PTASE11	0.182	−0.184	BAR	−1.362	1.610	INR
AT1G66145	CLE18	−0.570	−0.135	BAR	−1.422	1.680	INR

Table 2 Responsive and recovering genes absent from the ATH1 micro-array *(Continued)*

AT4G11485	LCR11	−0.969	−1.131	BAR	−1.695	1.849	INR
AT4G13890	SHM5	−0.177	−0.165	BAR	−1.534	1.421	INR
AT4G10767	SCRL21	−0.211	−0.470	BAR	1.459	−2.258	IPR
AT2G30432	TCL1	0.062	−0.924	BAR	1.680	−1.893	IPR
AT1G06280	LBD2	−0.667	−0.194	BAR	0.729	−1.385	LNR
AT4G29280	LCR22	−0.461	−0.171	BAR	0.485	−1.779	LNR
AT3G04430	NAC049	1.550	−0.809	BAR	0.731	−1.440	LNR
AT1G23147	RALFL3	−0.093	−0.201	BAR	1.262	−2.229	LNR
AT5G45875	SCRL27	0.864	0.235	BAR	0.754	−1.712	LNR
AT4G31380	FLP1	0.549	−0.073	BAR	−0.234	1.555	LPR
AT4G29283	LCR21	−1.583	−0.275	BAR	0.150	1.783	LPR
AT2G14935	LCR40	0.461	0.290	BAR	−0.469	1.423	LPR
AT2G12465	LCR50	0.500	−1.178	BAR	−0.942	1.510	LPR
AT2G02147	LCR73	0.599	1.466	BAR	−0.563	1.383	LPR
AT2G04425	LCR82	1.334	0.118	BAR	−1.264	1.380	LPR
AT4G36950	MAPKKK21	0.228	−0.210	BAR	−0.776	1.478	LPR
AT5G44430	PDF1.2 C	0.682	−1.123	BAR	−0.528	1.747	LPR
AT2G05117	SCRL9	−0.182	0.668	BAR	−1.005	1.595	LPR
AT5G37415	AGL105	0.684	−0.214	BAR	−1.931	0.608	PNR
AT2G45110	EXPB4	−0.018	0.286	BAR	−1.495	0.106	PNR
AT1G07900	LBD1	−0.174	−0.103	BAR	−1.834	0.837	PNR
AT3G43083	LCR33	−0.830	0.966	BAR	−1.956	0.748	PNR
AT4G39917	LCR45	−0.321	0.020	BAR	−1.897	0.452	PNR
AT5G14490	NAC085	0.099	−0.557	BAR	−1.365	0.724	PNR
AT4G11653	RALFL29	−0.280	−0.607	BAR	−1.900	0.762	PNR
AT1G60625	RALFL6	−0.668	0.726	BAR	−1.671	0.373	PNR
AT4G24230	ACBP3	1.295	−0.391	BAR	1.546	−1.194	PPR
AT4G29273	LCR23	0.128	−0.851	BAR	1.352	−0.802	PPR
AT2G19020	RALFL10	−1.217	0.276	BAR	1.745	−1.112	PPR
AT2G34825	RALFL20	0.240	0.456	BAR	1.375	−0.603	PPR
AT5G08150	SOB5	1.213	−1.337	BAR	1.944	−1.205	PPR

This table presents 71 of the 477 tiling-array-specific genes identified as differentially expressed during the P_i^{starv} response and/or recovery. These 71 were chosen only for the reason that they have been annotated with a gene symbol. The remaining 406 genes do not have gene symbols and are poorly annotated. See Additional file 5 for a complete list. *: Abbreviations for response (Res.) and recovery (Rec.).

P_i^{starv}. Thus, each phase may include genes that were either positively or negatively regulated. In this section we focus on genes that were root P_i-responders but not members of the group of 84 genes previously known to be P_i-responsive. Hence, all gene counts have been adjusted to exclude known P_i-responders. Genes that were responsive in the root's initial response phase consisted of 292 positively (IPR) and 112 negatively (INR) regulated genes whereas those persistently responsive included 45 positively (PPR) and 48 negatively (PNR) regulated genes. Finally, the root's latent response phase consisted of 423 positively (LPR) and 311 negatively (LNR) regulated genes.

To ascertain function, classified genes were annotated with GO-SLIM terms by which initial, persistent, and latent gene groups were annotated with 398, 146, and 665 functional terms, respectively. tMeV software [16,17] was employed to cluster functionally similar genes (Figure 4a (initial), 4e (persistent), 4i (latent)). Using functional-clusters we determined if gene members of any one functional-cluster displayed a stronger response than those of any other. To this end, we overlaid expression
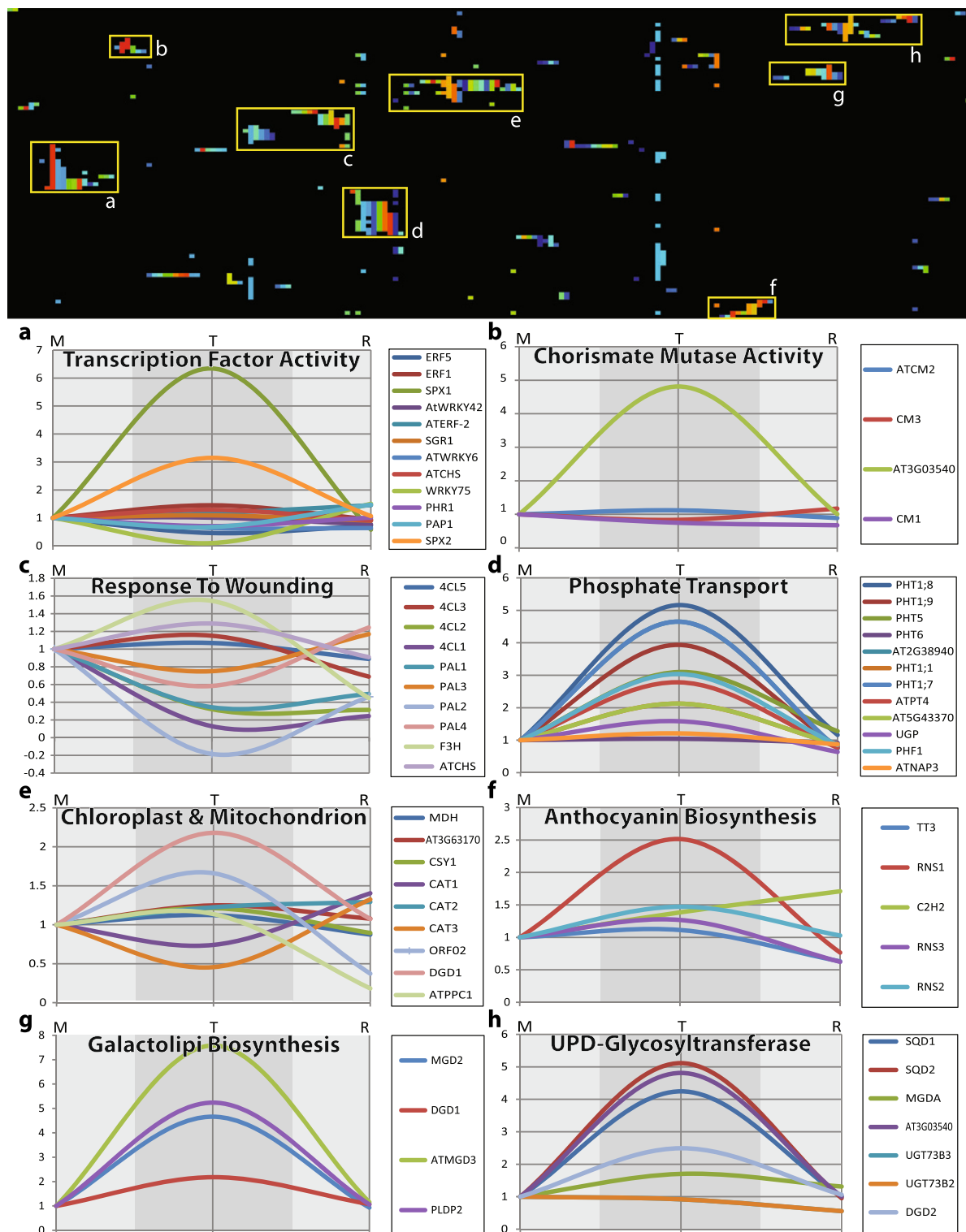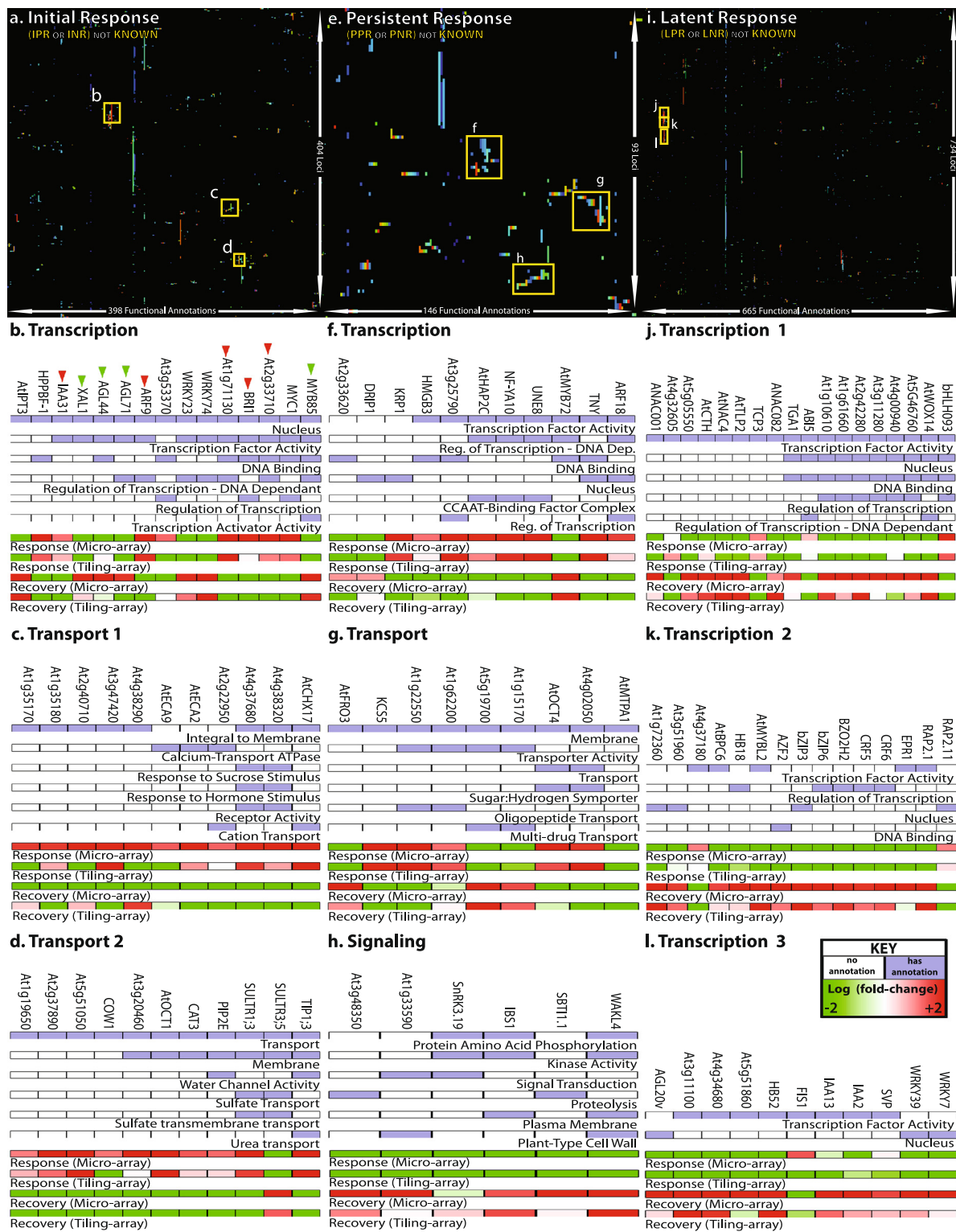
Figure 3 Analysis of gene expression and function among known P$_i$-responsive loci. (Top) Clustered heatmap of known P$_i$-responsive loci (rows) and GO-SLIM annotations (columns). Each color represents a different functional annotation and colors are only displayed, per row: if the rows gene is annotated by the GO-SLIM term. Selected clusters are marked from **a**-to-**h**. (Bottom, a-h) Transcription profiles of each functional cluster displaying the relative abundance of transcripts for particular known P$_i$-responsive genes in mock (M), treatment (T), and recovery (R) samples.

Figure 4 Analysis of gene expression and function among novel P$_i$-responsive loci. (Top, a, e, i) Clustered heatmaps of novel P$_i$-responsive genes (rows) and GO-SLIM annotations (columns) separately displayed for the initial (**a**), persistent (**e**), and latent (**i**) responses. (**b-d, f-h, j-l**) Summaries of selected clusters from clustered heatmaps showing annotations (blue: annotated; white: not annotated) and fold-change for response-and-recovery (red: positively regulated; green: negatively regulated) as measured by micro- and tiling-array platforms.

data with the heatmaps produced by tMeV (Figure 4). Figure 4 displays the results for each gene expression phase by highlighting results from the initial phase in the left column (Figure 4b-d), the persistent phase in the middle column (Figure 4f-h) and the latent phase in the right column (Figure 4j-l). Three prominent functional clusters were highlighted for each phase: Genes were displayed across columns, functional annotations were shown as rows, and gene expression was indicated for both micro- and tiling-array root datasets.

Initially responsive gene clusters generally performed functions in "transcription regulation" (Figure 4b), "ionic transport" (Figure 4c), and "transmembrane transport" (Figure 4d). Among the transcription factor (TF) genes identified, *AGL44, AGL71, XAL1(AGL12), MYB85*, and *WRKY23* were significantly down-regulated in roots (Figure 4b-green arrow). The agamous-like (AGL) TFs are known to be involved with root morphological processes [18], SOC1 is known to interact with both AGL44 and XAL1 [19], and MYB85 regulates lignin biosynthesis [20,21]. On the other hand, *ARF9, BRI1, IAA31, At1g71130*, and *At2g33710* were up-regulated (Figure 4b-red arrow). Both *At1g71130* and *At2g33710* are members of the *ERF/AP2* family with *At1g71130* being involved in sugar:phosphate studies and *At2g33710* in salt-stress. Thus, among others mentioned, *At2g33710* encodes a TF candidate gene that deserves further studies with regards to its role in P_i-signaling. The second cluster of ionic transport genes were all up-regulated in roots in response to P_i^{starv}. Three gene members of this cluster (*ECA9, ECA2, At2g22950*) encode proteins involved in calcium ion transport. *ECA9* is an auto-regulated Ca^{2+} efflux pump and the *ECA2* ATPase catalyzes Ca^{2+} efflux. Similarly, *ATCHX17* is a sodium/proton anti-porter and the gene for this protein was expressed 6.4 fold higher in P_i^{starv} than in the control, subsequently reducing its expression level by 5 fold during recovery. The third cluster included up-regulated genes encoding transporters. Most notably, genes for the sulfate and carnitine transporters, *SULTR1;3* and *OCT1*, were up-regulated by 7 and 71.5 fold in P_i^{starv}, respectively. Indeed, *OCT1* represented the most differentially expressed gene locus in this study.

Gene loci observed as persistently responsive were generally involved in "transcription regulation" (Figure 4f) and "ionic transport" (Figure 4g). These two functions were common to those seen among the initially responsive gene loci. However, a new function was also seen: "intracellular signaling" (Figure 4h). Of the TF genes (Figure 4f), *MYB72* was the most differentially regulated locus in root (7 fold). This was followed by *At3g25790*, a putative MYB transcription factor (TF), which was up-regulated by 3.5 fold. The ethylene responsive TF gene, *TNY (DREB A-4)*, exhibited a PPR expression pattern. It is involved in cytokinin biosynthesis [22], and cytokinin signaling is known

to cross-talk with P_i^{starv} signaling [23]. Additionally, the *DRIP1* gene identified as a member of the PNR class, encodes an E3 ligase known to mediate ubiquitination of *TNY*'s family member *DREB2A* [24]. Finally, three CCAAT-binding TF genes were significantly up-regulated: *NF-YA3* (HAP2C, 1.8 fold), *NF-YA2* (HAP2B, 2.5 fold) and *NF-YA10* (2.4 fold). The second persistently responsive gene cluster included genes coding for membrane-associated transport proteins (Figure 4g). *MTPA1*, a zinc-ion efflux transporter, was the most differently expressed in root (down-regulated by 10.2 fold). The gene for the iron-reductase, *FRO3*, also displayed a persistent negative response of 2.8 fold. By contrast, two peptide transporter genes, *At1g62200* and *At1g22550*, identified as members of the PPR class, have been implicated in zinc hyper-accumulation. And, the gene for another carnitine transporter, *OCT4*, displayed a PPR pattern with a 2.5 fold increase in transcript levels. In contrast to *OCT1*'s IPR pattern (fold-change of 71.5), *OCT4* did not return to basal expression levels during the recovery. The third persistently responsive gene cluster contained a mix of terms related to molecular signaling (Figure 4h). All genes within this cluster were negatively regulated and did not recover after 3 days in the replete medium. The most prominent members were *WALK4* (3.4 fold down-regulated) and *CIPK22* (3.3 fold down-regulated). The former encodes a member of the membrane-bound receptor-like kinase super family whereas *CIPK22* encodes a protein known to associate with calcium-binding calcineurin B-like proteins [25]. Finally, *At1g33590* which is involved in signal transduction and the karrikin response was persistently down-regulated by 2.6 fold [26].

Among the latently responsive gene loci the most prominent expression patterns belonged to clusters implicated in transcription regulation. In total, we identified 48 TF genes that were differentially expressed in roots during the recovery from, but not the response to starvation. This number exceeded the number of TF genes identified in the initial and persistent root response by 4 and 5.3 fold, respectively. Among proteins encoded by these 48 TF genes, several TF families were prominently represented: (1) the major leucine zipper family including 5 *bZIP*, 5 *bHLH*, 2 *WRKY*, and 2 *HB* TFs; (2) the *ERF/AP2* family, with 5 TFs; (3) the zinc finger family, with 4 TFs; and (4), the *NAC* family, with 3 TFs. The remaining 22 TF genes were distributed among those encoding *MYB, WUS, IAA*, and other families. Of the first family of major leucine zippers, 14 were distributed across *bZIP, bHLH, WRKY*, and *HB* sub-families. Members of the *bZIP* family are often involved in oxidative and pathogen defense responses and are commonly linked to ABA-related pathways [27,28]. In this group, genes for *BZIP3, BZIP6, BZIP9*, and *BZIP24* were differentially regulated in root during recovery from, but not response to P_i^{starv}. The *bHLH* gene family which

is generally involved in plant development, circadian rhythm, and stress [29] included genes for *BHLH093*, *MYC3*, *At1g10610*, *At1g61660*, and *At2g42280*. The WRKY family members which mediate salicylic and jasmonic acid signaling are involved in defense against pathogens and/or herbivores [30]. We found *WRKY7* and *WRKY39* to latently respond to P_i^{starv}. Finally, we identified *HD-ZIP18* and *HD-ZIP52* as two latently responsive genes. The second family of ERF/AP2 TFs are involved in acclimation stress responsive to salicylic acid, jasmonic acid, cytokinin, and ethylene [31,32]. Here, we identified 2 cytokinin response factors including *CRF5* and *CRF6* whose genes were up-regulated during the recovery period. Genes for 3 ethylene response factors, *RAP2.1*, *RAP2.11*, and *HRE1*, were found to express differentially during recovery. Members of the third major TF gene family encode zinc-fingers, of which we identified 4 positively regulated candidates, *ZF2*, *AT4G00940*, *ATCTH*, *GATA3*. The final pertinent TF genes identified were 3 members of the *NAC* family, *NAC001*, *NAC080, and NAC082*, which were also up-regulated in a similar manner.

The functional diversity across the latently expressed TF gene families prompted us to attempt to identify common processes among them. To this end we employed the TAIR database that provides associations of peer-reviewed articles to genomic loci described within said articles. Collating articles associated to latently expressed TF genes, we used a simple text-mining approach to group TF genes by previous research (see Additional file 8). We found 10 TF genes (*BZIP9*, *CRF6*, *MYBL2*, *NAC001*, *TGA1*, *ZF2*, *At1g61660*, *At2g03470*, *At4g32605*, *At4g37180*) previously identified in studies on pathogen response and cell-cycle regulation during geminivirus infection [33]. A separate set of 7 TF genes (*MDB2*, *TLP2*, *ZF2*, *At1g08170*, *At2g03470*, *At3g11100*, *At4g37180*) previously implicated in pollen germination and tube growth were latently regulated in roots [34]. Furthermore, 5 latently responsive TF genes (*BHLH093*, *BZIP9*, *HB52*, *RAP2.1*, *TLP2*) were reported in a cold-acclimation study [35]. Additional smaller groups of TF genes were identified in publications investigating topics such as "primary and secondary metabolites" [36], "post-transcriptional regulation" [37], "sucrose" [38,39], and "basal resistance to pathogens" [40]. Many TF genes were found to be shared across several studies. Together, these results suggested novel roles for these TF genes in roots during recovery from P_i^{starv}. On the other hand, they also highlighted the importance to consider which P_i-responsive genes were P_i-specific or non-specific. In the following section, we addressed these issues for all differentially regulated genes by comparing our results with those published by the AtGenExpress initiative.

Interaction between P_i-responsive genes and those responsive to various AtGenExpress treatments

We defined interaction as a gene differentially regulated in at least 2 treatments. With differential regulation being determined by statistical significance ($\alpha = 0.001$, using Bonferroni correction for multiplicity). To analyze possible interactions between the P_i response and several hormonal, environmental, and nutritive treatments, we constructed a network using the following steps: (1) We analyzed datasets from various AtGenExpress treatments (with ≥ 2 replicates) using the same methods and software as those for the analysis of our P_i dataset (i.e. a Bonferroni-corrected *p-value* of ≤ 0.001 versus respective control); (2) Genes differentially regulated in our root experiments were associated to AtGenExpress treatments for which they were differentially expressed; (3) We then weighted each gene-node by the number of treatments it was found to be differentially regulated and each treatment-node by the number of P_i-responsive genes found to be differentially regulated by that treatment. In this way, the network (Figure 5a) represented the degree to which genes interact with other treatments and which treatments elicit similar regulons to those initiated by P_i^{starv} in the roots. Thus, we described: (1) genes found to be specific to P_i^{starv} with no interaction among the treatments studied (Figure 5b-P_i Specific); and (2) highly interactive genes providing evidence for co-regulation (Figure 5b).

Gene loci specifically regulated during P_i^{starv} only

The following analysis was based on transcript abundance, therefore, Affymetrix probe-sets were used to represent genes and not AGI identifiers. By selecting a Bonferroni corrected *p-value* threshold of 0.001, we sorted 1249 root P_i-responsive genes (Affymetrix probe-sets) into either P_i-specific or non-specific bins (Figure 5b). Although there were actually 1257 root P_i-responsive genes, 8 ambiguously mapped to AGI identifiers and were discarded from further analysis. Approximately 70% of the 1249 genes were P_i^{starv} specific in roots, i.e. 869 genes were either initially (24%), persistently (5%), or latently (41%) responsive to P_i^{starv} and did not interact with those affected in other AtGenExpress treatments.

The P_i-specific genes included those already known to be P_i-responsive and those that were novel factors of P_i^{starv} response identified here. At a corrected *p-value* ≤ 0.001, 28 known P_i-responsive genes tended to be exclusively regulated by P_i^{starv}. Because this type of Boolean analysis did not distinguish between genes in terms of their specificity, we ascertained the minimum threshold (*p-value*) required to reclassify a P_i-specific gene as being non-specific (Figure 5d). The higher the *p-value* required, the greater the gene's specificity to P_i^{starv}. Therefore, by
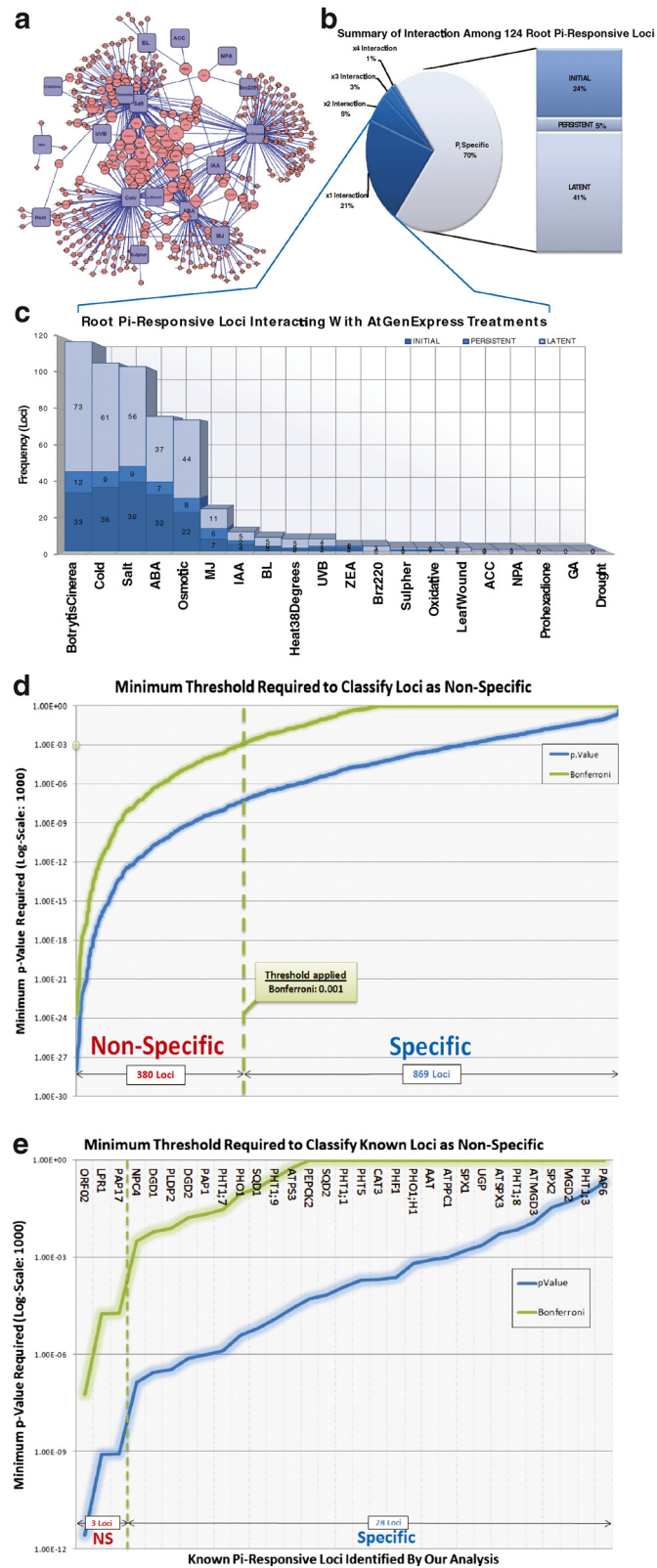
Figure 5 (See legend on next page.)

(See figure on previous page.)
Figure 5 Comparative analysis between P$_i^{starv}$ data and AtGenExpress. Subfigure (**a**) depicts a network of interactions between several types of treatment (blue squares) and genomic loci (other nodes) represented by probes on the ATH1 micro-array. Edges/lines are drawn between treatments and loci if the locus is differentially regulated in the treatment as compared to its control (see Additional file 9). (**b**) A pie chart summarizing the degree to which loci were found to interact with AtGenExpress treatments. Seventy percent of P$_i$-responsive loci are found to interact with nothing else, whereas 21% interact with 1 other AtGenExpress treatment and 1% interact with 4 AtGenExpress treatments. (**c**) Stacked histogram breaking down the degree of interactivity in terms of locus counts (y-axis) between various AtGenExpress treatments (x-axis). From bottom-to-top the stacked bars indicate the contributions made by the initial, persistent, and latent responses. (**d**) A plot describing the minimum threshold required (y-axis; *p-value*: blue; corrected: green) in order to detect a locus (x-axis; ranked by y-axis) as being differentially regulated in at least 1 AtGenExpress treatment. A dotted green line indicates the default threshold used by our analysis that results in 380 loci being detected in at least 1 AtGenExpress treatment and are therefore classified as non-specific. (**c**) A plot identical to (**d**), except only a subset of loci (x-axis) that are known to be P$_i$-responsive are displayed.

ranking each gene according to this minimum *p-value* threshold, we could compare their relative interaction. For instance, among the known set of genes, we found *PHO1*, *PHO1;H1*, *DGD1*, and *PHF1* to be specifically regulated in response to P$_i^{starv}$ (Figure 5e). We also observed that *PAP6*, *PHT1;3*, and *MGD2* ranked higher than any other known P$_i$-responsive genes and were therefore relatively more specific to P$_i^{starv}$ than to any other treatments tested. Indeed, *PAP6* displayed the most specificity to P$_i^{starv}$, requiring a notably relaxed threshold (*p-value* $\leq$ 0.2) in order to be classified as non-specific. Given the tendency of known P$_i$-responsive genes to include multiple members of the same family (such as ion-transporters), we were able to ascertain the relative specificity of the family members (Figure 5e): (1) Among the *PHT1* P$_i$-transporter family members, genes for PHT1;3 (42nd most P$_i$-specific), *PHT1;8* (226th most P$_i$-specific), *PHT1;1* (503rd), *PHT1;9* (637th), and *PHT1;7* (726th) were all P$_i^{starv}$ specific; (2) Among the lipid processing families, both *MGD2* and *MGD3* were highly ranked at 82nd and 189th, respectively, whereas, *DGD2* and *DGD1* were less specific with ranks of 760 and 811, respectively; (3) Three members of the *SPX* gene family were highly ranked at 330 (*SPX1*), 246 (*SPX3*), and 114 (*SPX2*); finally, (4) *PHO1*, a well-studied gene, was less specific (ranked 684th) than its close homolog, *PHO1;H1* (ranked 394th).

After ranking all P$_i$-responsive genes in our study (see Additional file 10), we found that several hundred P$_i$-responsive genes identified here were more specific to P$_i^{starv}$ than many genes previously reported as being P$_i$-responsive. For example, the top 100 most P$_i$-specific genes included only 3 members previously described as being P$_i$-responsive. These 3 were *PAP6* ranked 7th, *PHT1;3* ranked 42nd, and *MGD2* ranked 82nd. The remaining 97 genes responded to starvation in either an initial (49 genes), persistent (10 genes) or latent (38 genes) manner. The most P$_i$-specific and initially responsive genes included *At4g19770* (encoding a putative chitinase, responding at 3.5 fold and recovering at 4.3 fold) ranked 1st, *At4g25160* (encoding a receptor-like cytoplasmic kinase with similarity to universal stress response protein of

bacteria, responding at 7.5 fold and recovering at 16.5 fold) ranked 3rd and *At1g04700* (encoding a tyrosine kinase, responding at 1.8 fold and recovering at 2.2 fold) ranked 5th. Genes that persistently responded to starvation during recovery include *MTPA1* (encoding a zinc transporter, responding at 10.2 fold) ranked 2nd, *At3g53770* (encoding a LEA3 family member, responding negatively at 3.8 fold) ranked 6th, and *MYB72* (encoding a TF mediating systemic resistance, responding negatively at 7.3 fold) ranked 8th. Finally, the top most specific latently responsive genes included *At1g62090* (encoding a pseudogene-protein kinase, recovering negatively at 1.6 fold) ranked 10th, *At5g66220* (encoding a chalcone-flavanone isomerase, recovering negatively at 1.6 fold) ranked 12th, and *At3g26130* (encoding a cellulase, recovering at 1.8 fold) ranked 13th.

P$_i$-responsive genes co-regulated in multiple AtGenExpress treatments

Approximately 70% of the 1249 P$_i$-responsive genes in roots identified here were P$_i$-specific at a *p-value* $\leq$ 0.001. There was no detectable response of these genes among any AtGenExpress treatments covering stimuli ranging from hormonal and nutritional to environmental. The remaining 30% of genes (380) were not considered P$_i$-specific because they differentially responded with up to 4 additional treatments found in AtGenExpress. We exploited this behavior in an attempt to elucidate: (1) treatments displaying the most similarity to P$_i^{starv}$ in terms of differentially regulated genes; (2) gene interaction and regulation by hormonal treatments; and (3) cohorts of co-regulated genes.

To determine which treatments were most similar to P$_i^{starv}$, we considered only those genes significantly regulated. We counted the frequency of genes differentially regulated in both P$_i^{starv}$ and each AtGenExpress treatment. We then weighted treatment-nodes by this frequency and ranked them (histogram, Figure 5c). Our results showed that *Botrytis cineria* infection (118 common genes) followed by cold (106), salt (104), and osmotic (74) stress

treatments were most similar to P_i^{starv}. Furthermore, most genes interacting with these treatments were latently responsive in our experiments, and were mostly associated to one other non-P_i-related treatment. We found that the maximum degree of interaction displayed by any P_i-responsive gene was 4 AtGenExpress treatments (Figure 5b, Figure 6a-d).

Among the hormone treatments tested (ABA, ACC, BL, GA, IAA, MJ, and ZEA) ABA treatment with 76 common genes displayed the most interaction with P_i^{starv}. After which, the frequency declined sharply to MJ treatment (24 common genes), IAA treatment (11), BL treatment (8), ZEA treatment (3), ACC treatment (1) and GA treatment (0). Close inspection of those P_i-responsive genes associated with ABA treatment uncovered many genes related to cold, salt, and osmotic treatments (Figure 6a-d). Of the 10 genes interacting with ABA, cold, salt, and osmotic treatments, only *AZF2, CYP706A2, SPS2F,* and *TRI* have been annotated in public databases. Not surprisingly, salt and osmotic treatments shared several responsive genes; these genes were also P_i-responsive and included *AAP1, MYB74, and SS2*.

Overall, inspection of the interaction-network uncovered clusters of co-regulated genes. The most central cluster of genes consisted of those associated with treatments most similar to P_i^{starv}. These genes included *AZF2* (zinc finger protein, known to be regulated by ABA, salt, and desiccation), *SP2F* (putative sucrose-phosphate synthase activity), *TRI* (tropinone reductase), *At1g52560* (HSP20-like), *At1g62570* (Flavin-Monooxygenase family implicated in multiple-stress studies), *At3g01260* (Galactose-mutarotase family), and *At5g35735* (Galactose-mutarotase family). These clusters of interacting genes suggest co-regulatory mechanisms and may therefore lead to the discovery and/or elucidation of possible novel P_i-responsive network.

Discussion

High-throughput technologies recently applied to studying P_i^{starv} in Arabidopsis have contributed to the overall understanding of how plant molecular systems react to P_i-limiting stress [9-14]. However, comparing results from these studies is problematic due to different experimental designs. For example, Misson et al. (2005) [9] focused on leaf and root tissues, whereas Muller et al. (2007) [11] examined shoot tissues; Muller et al. (2007) additionally studied those genes that interact with pathways evoked during sucrose limiting stress. These studies shared the overall strategy to investigate a plant's initial responses to P_i^{starv}. Only one high-throughput study has thus far characterized the molecular response during recovery from P_i^{starv} [10]. This work demonstrated that a subset of genes found to respond to P_i^{starv}

by prior research could also recover and thus identified high-confidence candidates sensitive to P_i-flux. Together, these four studies have significantly increased our current understanding of P_i^{starv} on a genome-wide scale. This report furthers the knowledge garnered by those four reports described above by combining their experimental designs under a single framework. Hence, the data described here offers insights into areas previously unreported, such as the transition between the initial response and the latent recovery phases, the detection of organ-specific differences in gene regulation and the combination of both to define the systemic plant response.

Thirty-six organ- and response-specific arrays were analyzed with the initial aims of generating a reference dataset for molecular responses to P_i^{starv} to provide additional insights for those responses and to identify new P_i-responsive candidate genes. To manage this dataset, a classification scheme was designed to broadly categorize novel response-and-recovery gene expression patterns. Using this scheme a unique and comparably large molecular response was identified in roots relative to shoots. We analyzed the interaction of P_i-responsive genes with several hormonal, environmental, and nutritive treatments. This exercise defined non-specific P_i^{starv} genes differentially regulated across multiple stimuli; in particular, stimuli such as cold, osmotic, and salt stress. Furthermore, the hormone ABA appeared to regulate substantially more P_i-sensitive genes than other hormone treatments. This supports the premise that of the hormone regulators ABA is likely a key player during P_i-flux. Significantly, the majority of genes known to respond to P_i^{starv} were observed to be regulated by several different treatments. Thus, this known gene-set that includes many well described P_i^{starv}-sensitive genes such as *PHO1* is indeed not P_i^{starv}-specific. To place this into context we note that many genes not previously identified as P_i-responsive, but identified as responsive here exhibit a lesser degree of cross-talk and hence occupy roles that are relatively more P_i^{starv}-specific. This insight provides opportunity for both generating and addressing additional questions regarding the regulation of molecular networks during nutrient stress. Given the nature of genome-wide technologies employed here much depends on the wealth of knowledge and annotations generated by prior researchers studying several genes using non-high-throughput methods. Therefore, a thorough literature and database survey was conducted for both those genes known to respond to P_i^{starv} and those additional genes observed during the course of this study. Thus, we were able to report on all results in the context of novel findings by examination of candidate genes and their corresponding gene expression patterns during the response and recovery.
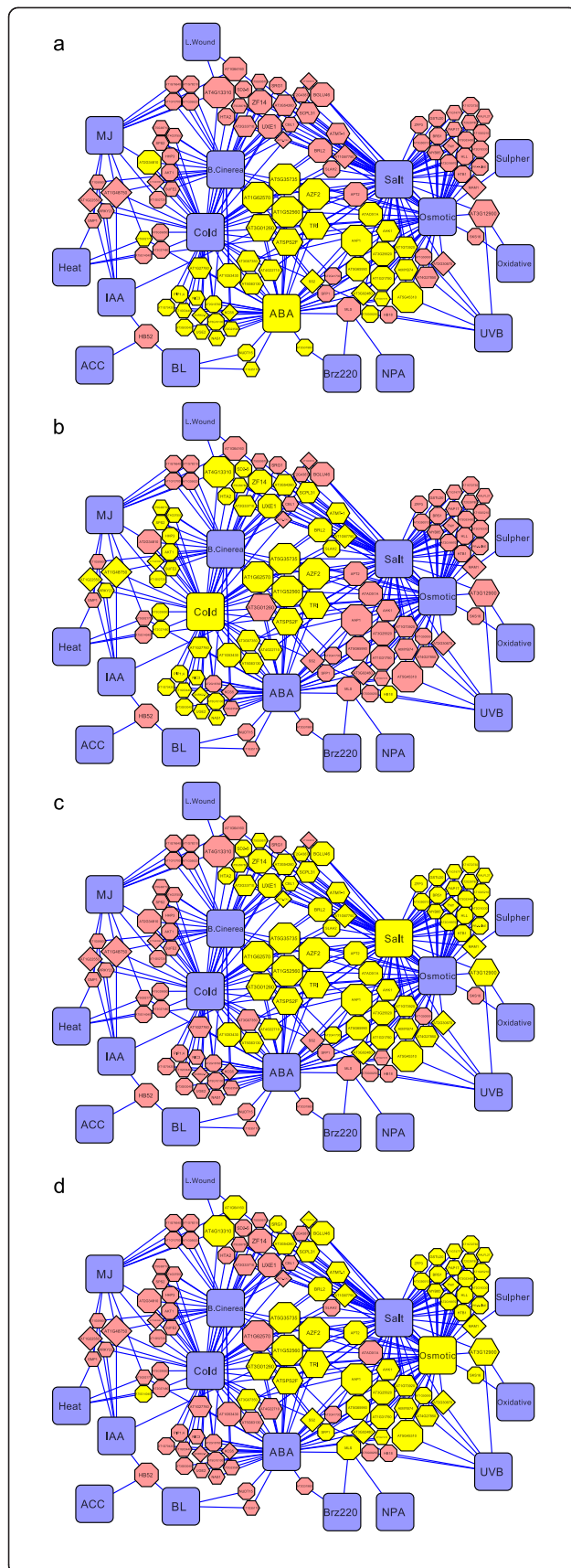
Figure 6 Cross-talk between P$_i^{starv}$, ABA treatment and cold, salt, and osmotic stress. Subfigures (**a**) through (**d**) display highlighted portions of Figure 5a. P$_i$-responsive loci are highlighted (yellow) if they have additionally been found to be regulated by ABA treatment (**a**), cold stress (**b**) salt stress (**c**), and/or osmotic stress (**d**). The degree of overlap between highlighted regions is high indicating a large degree of cross-talk between treatments.

Comparisons among different studies reveal the need to establish a reference dataset

Although previous experiments by various groups have, in aggregate, reported a total of 84 P$_i$-responsive genes, our work here has observed 40% of these genes being responsive to starvation and recovery treatment. As this appeared to be a small proportion we addressed this issue by analyzing the benchmark set by previous genome-wide experiments: Misson et al. (2005) [9], Morcuende et al. (2006) [10], Muller et al. (2007) [11], and Nilsson et al. (2010) [12] each identified 14%, 33%, 3%, and 8% of the 84 significantly responsive genes, respectively. Therefore, due to the lack of overlapping results, it appears that the core set of known P$_i$-responsive genes is highly variable and most likely dependent on the experimental approach. This between-study variation highlights the need to standardize experimental designs and to ascertain the cause behind the regulation of core P$_i$-responsive genes.

Among 33 of the known 84 P$_i$-responsive genes identified, the majority (75%) were found to be initially responsive and their expression returned to basal levels during recovery. Only 24% of the genes were latently responsive and the remaining 1% was persistently responsive. We propose that the bias towards the initial response is due to prior research almost exclusively focusing on the starvation response without considering recovery. Thus, known P$_i$-responsive genes tend to be initially responsive. Only a few studies have examined recovery from starvation which is reflected by the lower proportion of known genes identified as being latently expressed.

Expression profiles of P$_i$-starvation responsive genes absent from the ATH1 micro-array

Even though the ATH1 micro-array lacks genome-wide coverage it has been widely used for transcriptome studies. Whereas the 1.0R tiling-array is not comprehensive it certainly interrogates more of the Arabidopsis genome than ATH1 and therefore has a distinct advantage. However, the public literature surrounding array-based studies is dominantly micro-array based. Analyses and methods using the micro-array architecture are better described and the genes represented by the ATH1 chip are, in general, better annotated. Therefore, given the goal of this study to better characterize the molecular

response and recovery to P_i^{starv}, the micro-array platform was chosen as the primary means to analyze gene expression. Nevertheless, our acquisition of tiling-array data in parallel serves to both corroborate micro-array results as well as to investigate the response and recovery of those genetic elements not represented by ATH1 probes. We have determined the response and recovery profiles for all 5,044 nuclear protein coding genes absent from the ATH1 micro-array (see Additional file 5) and detected 477 genes that may play a role during and post P_i^{starv} in roots and shoots (Table 2). Among those 477 genes we identified *IPS1* (now known as non-protein coding), *GDPD3* (a membrane-remodeling factor) and *CPL3* (a MYB TF), for which we describe their biology and response to P_i^{starv} below.

IPS1 is a P_i^{starv}-inducible non-coding RNA whose transcript level is regulated by a myb transcription factor, *PHR1* [41]. By a mechanism known as target-mimicry, *IPS1* is resistant against the activity of RISC-loaded miRNA399 due to its partial sequence complementarity to the mature miR399. This property enables *IPS1* the ability to quench the miR399 signal without being cleaved by the latter [42]. RT-PCR showed that the *IPS1* transcript level was inversely correlated to P_i availability in hydroponic media (see Additional file 4). This was also shown by tiling-array analysis of roots and shoots for which the responses ($Log_2(P_i^{starv}/P_i^{mock})$) were 6 and 6.5, respectively. The *IPS1* expression profile was the most differentially regulated profile among the 5,044 tiling-array-specific genes examined. Given the established role of *IPS1* during P_i^{starv}, this gene represents an excellent positive control for the remaining 476 genes identified by the tiling-array platform alone.

Unlike *IPS1*, the glycerophosphodiester phosphodiesterase (GDPD) gene family member, *GDPD3*, was not implicated in P_i homeostasis until 2011 [43]. Our tiling-array data corroborated this result as *GDPD3* (*At5G43300*) exhibited a 19 fold increase in signal intensity during the P_i^{starv} response in roots. The function of the GDPD family has been implicated in P_i-recycling through a membrane remodeling process that is sensitive to P_i-flux. Together with the vacuole, phospholipid bilayers are a major reservoir of internal cellular P_i. Membrane remodeling is a physiological response of plant cells to supply P_i on demand. This method of P_i-recycling replaces phospholipids in internal cellular membranes with alternate forms such as galacto- and sulfo-lipids [44,45]. GDPD hydrolyzes glycerolphosphodiesters originating from phospholipids and produces a glycerol-3-phosphate (G-3-P) and a corresponding alcohol. The G-3-P byproduct is further degraded by acid phosphatases resulting in P_i accumulation [43]. This remodeling mechanism is one example of a plant-wide response to P_i-limitation at a micro-scale, in addition to responses at the macro scale, e.g. by remodeling root architecture.

Plasticity of root architecture is related to the availability of soil nutrients under fluctuating environmental conditions. Under P_i-limiting conditions, root architecture changes by inhibiting primary root growth and promoting increased density of both lateral roots and root hairs [46]. Cell fate of epidermal trichoblast and atrichoblast is specified by several negative cell and non-cell autonomous regulators *GL2*, *CPC*, *TRY*, and *ETC*s [46]. On the other hand, *CAPRICE LIKE MYB3* (*CPL3*) has been characterized as a positive regulator for root hair patterning [47]. Since *CPL3* is not represented by ATH1 probes and hence unlikely to be described in previous studies of P_i starvation, we were interested to gauge this gene's response and recovery from our tiling-array data. Indeed, *CPL3* was initially up-regulated by 19.6 fold in roots and returned to basal levels during recovery (IPR). Whilst less remarkable the shoot response also displayed an IPR pattern of gene expression exhibiting an initial fold-change of 2.8. Therefore, the P_i^{starv} response may involve *CPL3* to govern root hair patterning. Our identification of *CPL3*, *GDPD3*, *IPS1*, and the other 474 genes as being P_i^{starv}-responsive exemplifies the utility of tiling-arrays in P_i^{starv} studies with regards to discovering new candidates for future research.

A novel root response suggests roles for energy metabolism and ionic transport

Previous P_i^{starv} research has not yet addressed root responses from the perspective of genome-wide studies. Whereas whole seedling experiments have undoubtedly captured a part of the root's responses, the results are likely skewed towards shoot responses as we have found that in 2 week old seedlings the average root to shoot RNA-abundance ratio is 1:9 (data not shown). Here, we found that the number of responsive genes in roots was 6.9 fold higher than those in shoots. Additionally, the distribution of genes in terms of fold-change in their response-and-recovery highlights greater responses to P_i^{starv} in roots than shoots (Figure 1). Furthermore, only 7% of P_i-responsive genes in roots were significantly altered in shoots. These 3 observations emphasize the importance of a global analysis of the root-specific response which hitherto has been neglected. To better understand the root response, we divided all root responsive genes into 1 of 3 categories (initial, persistent, or latent), and selected 3 prominent (in terms of fold-change) clusters of functionally related genes per category. Among genes in the initially responsive category, the most prominent clusters were involved in ion and trans-membrane transport, specifically calcium and sodium ion transport (Figure 4c,d). Whereas, the third prominent cluster grouped genes functioning in transcription regulation (Figure 4b).

We found lipid metabolism to play a role in the initial and persistent response. *OCT1* was co-identified with several membrane transporters in the initial response. *OCT1* exhibited the most fold-change of any gene observed before returning to basal levels during recovery. Similarly, *OCT4* was identified in the persistent category and while it did not recover it also did not display as dramatic a fold-change as *OCT1*. *OCT1* and *OCT4* encode carnitine transporters involved in mitochondrial fatty acid metabolism. Arabidopsis mutants deficient in *OCT1* and transgenic plants overexpressing *35 S::OCT1* have been shown to promote and suppress lateral root hair development, respectively [48]. Paradoxically, *OCT1* is up-regulated 71-fold during P_i^{starv}, but lateral root hair development is positively regulated during P_i-limitation. Thus, OCT1 appears to be uncoupled from root hair development during P_i^{starv} and may hypothetically play a role in P_i^{starv}-induced lipid/energy metabolism.

The root up-regulates transcription factors as the system tends toward recovery

Regulation of *AGL* expression occurred during the initial response but regulation of the *NF-YA* family members persisted after the recovery period, although the reason for this difference is presently unknown. Nevertheless, our results provide a shortlist of additional TF candidates for future research. Considering both the number of additional TF genes displaying initial and persistent responses, it is likely that the P_i^{starv} response is regulated by more than just the two TFs (*PHR1*, *PHL1*) identified to date [13,49] as previously corroborated [12,50]. Indeed, we observed a marked increase in the number of differently regulated TF genes (48 TFs) during the latent response, which increased by 4 and 5.3 fold from the number of TF genes observed during the initial and persistent responses, respectively. These results suggest that significant regulatory changes occurred latently during the period of recovery from P_i^{starv}. Using a text-mining approach we have uncovered some P_i-responsive TF genes to be involved in viral infection, cold acclimation and even pollen tube growth (PTG). Interaction of P_i-responsive TF genes with genes involved in viral defense and cold acclimation can be explained if a general stress response underlies all three cases. In addition, root hair extension is promoted during P_i^{starv} and is known to share many common features with pollen tube growth (PTG).

Expression of IPT3, ARF9, and MYB85 may alter root-morphology during P_i^{starv}

During P_i^{starv} the root architecture is significantly altered through both negative and positive regulation of primary and lateral root (LR) development. Root development processes are known to be down-regulated by cytokinin

(CK) at high concentrations [51]. Therefore, P_i^{starv} may be expected to reduce endogenous CK concentrations to release LR developmental pathways. Although CK concentrations were not directly measured in our experiments, we found a significant down regulation of *IPT3* in roots suggesting an additional P_i^{starv}-specific role for this gene in root CK biosynthesis.

Our results show an increased expression of *ARF9* in root tissues, although this gene has not yet been reported to play a role in root architecture nor in the P_i^{starv} response. However, *ARF9* is known to be up-regulated by high auxin concentrations similarly to its family members *ARF7* and *ARF19*, which promote LR formation in initiating cells accumulating auxin [52]. This shows that *ARF9* does have a role in P_i^{starv} and suggests that the role may be in morphological changes of root architecture.

Development of LR first entails the removal of structural scaffolds within cell walls, a process critical for cell expansion and proper root hair development. This process requires both the down-regulation of positive regulators (*MYB69* and *MYB85*) as well as an up-regulation of negative regulators. We found that *MYB69* and canonical upstream regulatory genes (*SIZ1, SND1, NST1, and VND6*) were all basally regulated during P_i^{starv} in roots. Yet, expression of *MYB85* (required for proper lignin deposition) was significantly reduced. This selective down-regulation of *MYB85* suggests attenuation of lignin deposition, resulting in a favorable environment for initiation of root hairs under P_i^{starv}.

Cross-talk among P_i^{starv} candidates uncovers interaction with plant hormones

To observe possible cross-talk between P_i^{starv} and hormonal responses we investigated interaction between our and relevant AtGenExpress data-sets. All AtGenExpress datasets were re-analyzed in the same manner as performed on our own. P_i-responsive genes were considered to be specific to P_i^{starv} if they were not differentially regulated in any treatment regime. Hence, by determining the minimum *p-value* threshold required for each gene to be categorized as non-specific we were able to rank each P_i-responsive gene and determine its relative specificity. Using this method we showed that *MYB72* is highly P_i-specific when compared to any other gene. This measure of relative specificity allowed us to determine which members of gene families play a primary role and which are functionally redundant in the P_i-response. Although both *MYB72* and MYB*74* are significantly regulated the former gene is ranked 8th for P_i-specificity whereas the latter 1238th. By contrast, all the 3 cytochrome P450 genes (*CYP94D1*, ranked 13th; *CYP735A1*, ranked 24th; *CYP76G1*, ranked 27th) were highly specific to P_i^{starv}. This result suggests that they are not redundant and execute distinct functions with little overlap. We note that this

analysis is heavily dependent on the number or breadth of treatments tested. To interpret highly P_i-specific genes, we have assumed the treatments selected from AtGenExpress to be an adequate sampling of biological stimuli.

In addition to specificity, we have also attempted to measure gene interaction. Highly specific genes may lose their specificity by inclusion of additional treatments to the study. On the other hand, the less specific a gene, the more interactive it becomes and the less likely it is to change when additional treatments are included in the study. Also, highly interactive P_i-responsive genes offer clues to P_i-signaling in terms of co-regulation. For instance, we have determined groups of co-regulated P_i-responsive genes that are influenced by one or more of the following treatments: ABA, cold, salt, drought, and *B. cinerea* infection. Indeed, these 5 treatments give the greatest degree of interactivity with P_i^{starv}. When compared to ABA treatment other hormone treatments such as ACC, IAA, MJ, BL, and ZEA elicit the expression of at most less than 32% of the number of P_i-responsive genes.

Conclusion

This study presents a genome-wide description of Arabidopsis' response and recovery to P_i^{starv} for both roots and shoots. Utilizing two different technological platforms to determine transcriptome changes we found that the majority of known P_i-responsive genes were initially responsive. Whilst our analysis mainly focused on genes represented by probes on both micro- and tiling-array platforms we also identified 477 tiling-array-specific genes as being regulated by P_i^{starv}. One such gene was *IPS1* a non-coding gene important for P_i homeostasis that exhibited an initial fold-change in roots and shoots of 63 and 95, respectively. For research areas such as plant P_i starvation, where transcriptomics studies have relied heavily on micro-array data, these results highlight the utility of true genome-wide studies in the detection of coding as well as non-coding transcript levels. All together, our results show a more varied response-and-recovery molecular phenotype than hitherto recognized in the literature. This study, which presents an initial investigation into the functional aspect of these P_i-responsive genes, has uncovered a progression of differentially regulated functional classes: from initially responsive ion-transporters and persistent cellular signaling genes to latently responsive transcriptional regulators. We hypothesize that initially responsive genes identified in this study function in immediate survival to P_i limiting stress – transporting P_i from source-to-sink whilst maintaining electrochemical gradients as indicated by the initial regulation of P_i and metal-ion transporters. This hypothesis is extended to include persistently and latently responsive genes whereby we surmise that persistently responsive genes participate in the transition between survival and recovery. This transition is evidenced by the increase in differential regulation of persistently responsive genes involved in cellular signaling to those latent genes coding for transcriptional regulators. Moreover, the extent of transcriptional regulators elicited by P_i^{starv} suggests the presence of regulons separate from that of the *PHR1* regulon. Whether or not these regulons are P_i^{starv}-specific remains an open question. However, analysis of cross-talk using data generated from this study and from AtGenExpress revealed that many novel P_i-responsive genes identified here appear to be more specific to P_i^{starv} than previously identified P_i-responsive regulons. Interestingly, *PHO1;H1* – a close homolog to *PHO1* with functional redundancy in P_i-signaling – showed less cross-talk with other treatments than *PHO1*, in roots. This suggests that even though *PHO1* traditionally displays a greater response to P_i^{starv} than *PHO1;H1*, the *PHR1*-mediated *PHO1;H1* response may be more specific to P_i^{starv} than the *PHO1* pathway (*PHR1*-independent). By applying the same reasoning to other well-known P_i responsive families we observed that: 1) genes involved in the biosynthesis of galactolipids (phospolipid alternatives) in non-photosynthetic tissues – *MGD2, MGD3*, and *DGD2* – were highly specific to P_i limiting stress; 2) P_i transporters *PHT1;1, PHT1;3* and *PHT1;7–9* (regulated by *PHR1*) were specific to P_i^{starv} whereas their other family members were not. Also, *PHT1;1* is regarded as one of the most responsive P_i transporters to P_i limitation suggesting that *PHT1;1* is the primary acting member of the *PHT1* family in the starvation response; 3) 3 of the 4 members in the *SPX* family are P_i^{starv} specific (*SPX1-3*). Interestingly, *SPX1-3* are under *PHR1* control. Indeed, for each of the known P_i responsive gene families mentioned, the members that we observed to be most P_i^{starv}-specific – *PHO1; H1, PHT1;7–9*, and *SPX1-3* – have also been reported to be regulated by the TF *PHR1*. Finally, a large degree of cross-talk among clusters of co-regulated genes implicated ABA as the likely hormone mediator responsible for regulating common stress-responsive pathways; in particular cold, salt, and osmotic stress. In the future we will apply this approach to the analysis of additional treatments with the view of building a comprehensive stress response-and-recovery database.

Methods

Plant material and growth conditions

Non-sterile WT (Col-0) seeds were sowed on rock wool (Grodan Inc.) pre-soaked in basal MGRL hydroponic media[24] and cold-treated at 4°C for 3 days. Plants were grown at 22°C under 150 μmol m^{-2} S^{-1} fluence rate and a 12 hr:12 hr light:dark cycle. To minimize environmental variation, plants were rotated in growth chambers once a day. In phosphate depleted media, 1.75 mM MES

(pH 5.8) was used instead of 1.75 mM sodium phosphate (pH 5.8). All hydroponic media were aerated to maximize air supply during hydroponic culture. All plants were grown in basal MGRL hydroponic media for 20 days before being transferred to a phosphate-deficient medium. During the 10-day treatment, the phosphate-deficient medium was replaced every three days. For recovery experiments, plants previously grown in phosphate-deficient medium for 10 days were transferred to full-strength MGRL medium for an additional 3 days. Samples were collected on the 10th and 13th (10 + 3) day. Phosphate-starved shoot and root samples were collected separately at the indicated time point. Furthermore, all experiment procedures such as media replacement and sample collection were performed in the middle of day in order to minimize possible circadian effect. In parallel, control plants were grown in a full-strength MGRL media before sample collection on the 10th day after the initial 20-day growth period.

Preparation of genechip and tiling-arrays

Total RNAs extracted by RNA easy extraction kit (Qiagen) were used for Arabidopsis Genechip ATH1 and tiling arrays 1.0R (Affymetrix). Samples included three biological replicates each for mock-treatment leaves (ML), mock-treatment roots (MR), P_i-starvation-leaves (TL), P_i-starvation-roots (TR), P_i-starvation-recovery leaves (RL), and P_i-starvation-recovery roots (RR). Probes of all 36 samples were synthesized as previously described[25,26]. The efficiency of biotin labeling was confirmed by Gel-shift assay with NeutrAvidin (Pierce) as described in Genechip Whole transcript (WT) double-stranded target assay manual (Affymetrix). Hybridization and scanning of all arrays were done at the Genomics Resource Center in the Rockefeller University following the manufacturer's instructions (Affymetrix).

Detection of phosphate responsive genes

Semi-quantitative RT-PCR and real-time PCR were performed to confirm expression changes of selective genes uncovered by gene/tiling arrays. Typically, 1 μg total RNA prepared by Qiagen RNA column extraction including DNase treatment (Qiagen) was used as a template for reverse transcription (Superscript III RT-PCR, Invitrogen). First strand cDNA was synthesized with an oligo dT primer or with an strand-specific primer. In parallel, *actin* transcript was used as an internal loading control and same amount of RNA without reverse transcription as a negative control. 100 ng of single strand cDNA were used to quantify expression by real-time PCR (Bio-Rad CFX96). Each $\Delta C(t)$ value and relative expression of phosphate-responsive genes was determined by Bio-Rad CFX manager program (Bio-Rad).

Description of gene lists

Below is a description of the pertinent gene lists mentioned in this work.

General statistics (based on transcript levels):

1. 1.1257 Affymetrix probe-sets differentially expressed in roots.
2. 182 Affymetrix probe-sets differentially expressed in shoots.
3. 89 Affymetrix probe-sets commonly regulated in roots and shoot.
4. 1350 Affymetrix probe-sets identified in total (root + shoot - common).

Functional analysis (based on one-to-one relationships for terms and AGI identifiers):

5. 84 AGI identifiers previously known as Pi responsive.
6. 1231 AGI identifiers in root response, excluding the 84 previously identified.

Cross-talk analysis (based on transcript levels):

7. 1249 Affymetrix probe-sets differentially expressed in roots.

   a. a.1257 minus 8 Affymetrix probe-sets which were ambiguously mapped to AGI identifiers and discarded from further analysis.

Bioinformatics

The accession code, GSE34004, may be used to access the micro- and tiling-array data from the Gene Expression Omnibus (GEO). The computational portions of the Materials and Methods are described in Additional file 9. This file includes descriptions of the: *analysis pipeline; experimental design; quality control; normalization; gene classification; analysis of functional annotations; and analysis of P_i^{starv} specificity and cross-talk.*

Additional files

Additional file 1: Inter-study comparison, is a figure detailing a comparison of genes identified by various research groups to be regulated by phosphate flux.

Additional file 2: Response and recovery (eBayes), contains statistical data generated from the ebayes function in the Limma package (R, statistical environment) for the response and recovery in both roots and shoots.

Additional file 3: qRT-PCR, is a figure displaying qRT-PCR results for 37 loci from the top differentially expressed genes known to respond to phosphate-starvation.

Additional file 4: P_i marker genes, RT-PCR of P_i-starvation responsive non-coding RNAs IPS, miR399, and miR827 at 10-days P_i-replete and -starved, and 3-days recovery.

Additional file 5: Expression profiles for 5,044 genes undetectable by the ATH1 micro-array platform, a table describing the response and recovery of said 5,044 genes to Pi starvation in both root and shoot.

Additional file 6: Literature survey references, additional references used in the determination of the 84 known Pi-responsive gene-set.

Additional file 7: Gene response and recovery class list, categorizes genes into 1 of 9 response-and-recovery classes for roots and shoots, separately.

Additional file 8: Textmining data, is a table providing the data we collected and used to mine the text resources annotated by TAIR for each locus.

Additional file 9: Materials and methods for Bioinformatics, the computational portion of the materials and methods section.

Additional file 10: P$_i$-specifity rankings, is a table summarizing results for loci that we were able to assign a ranking of phosphate-specificity.

Abbreviations
P$_i$: phosphate; P$_i^{starv}$: P$_i$ starvation; P$_i^{mock}$: mock treatment; P$_i^{replete}$: P$_i$ replete; PC: principal components; BAR: Basal Response; IPR: Initial Positive Response; INR: Initial Negative Response; PPR: Persistent Positive Response; PNR: Persistent Negative Response; LPR: Latent Positive Response; LNR: Latent Negative Response; CPR: Continuous Positive Response; CNR: Continuous Negative Response; RR: Root Response; SR: Shoot Response.

Competing interests
The authors declare that they have no competing interests.

Author's contributions
The experimental design was conceived by JW, TK, MH, and NHC and all experiments were performed by JW except the computational analysis. Data was analyzed by CRM with assistance from JL, HW, XJW, and VBB. This paper was written by JW, CRM, VBB, and NHC. All authors read and approved the final manuscript.

Author details
[1]Laboratory of Plant and Molecular Biology, The Rockefeller University, New York 10065, NY, USA. [2]Bayer Crop Science, Technologiepark 38, 9052, Ghent, Belgium. [3]State Key Laboratory of Plant Genomics, Institute of Genetics and Developmental Biology, Chinese Academy of Sciences, Beijing 100101, China. [4]Computational Bioscience Research Center (CBRC), King Abdullah University of Science and Technology (KAUST), Thuwal, Kingdom of Saudi Arabia.

References
1. Raghothama KG: **Phosphate Acquisition.** *Annual Review of Plant Physiology and Plant Molecular Biology* 1999, **50**:665–693.
2. Schachtman DP, Reid RJ, Ayling S: **Phosphorus Uptake by Plants: From Soil to Cell.** *Plant Physiology* 1998, **116**:447–453.
3. Vance CP, Uhde-Stone C, Allan DL: **Phosphorus acquisition and use: critical adaptations by plants for securing a nonrenewable resource.** *New Phytologist* 2003, **157**:423–447.
4. Ma W, Ma L, Li J, Wang F, Sisak I, Zhang F: **Phosphorus flows and use efficiencies in production and consumption of wheat, rice, and maize in China.** *Chemosphere* 2011, **84**:814–821.
5. MacDonald GK, Bennett EM, Potter PA, Ramankutty N: **Agronomic phosphorus imbalances across the world's croplands.** *Proc Natl Acad Sci U S A* 2011, **108**:3086–3091.
6. Chebud Y, Naja GM, Rivero R: **Phosphorus run-off assessment in a watershed.** *J Environ Monit* 2011, **13**:66–73.
7. Howarth R, Sharpley A, Walker D: **Sources of nutrient pollution to coastal waters in the United States: Implications for achieving coastal water quality goals.** *Estuaries and Coasts* 2002, **25**:656–676.
8. Moss B: **Water pollution by agriculture.** *Philos Trans R Soc Lond B Biol Sci* 2008, **363**:659–666.
9. Misson J, Raghothama KG, Jain A, Jouhet J, Block MA, Bligny R, Ortet P, Creff A, Somerville S, Rolland N, *et al*: **A genome-wide transcriptional analysis using Arabidopsis thaliana Affymetrix gene chips determined plant responses to phosphate deprivation.** *Proc Natl Acad Sci U S A* 2005, **102**:11934–11939.
10. Morcuende R, Bari R, Gibon Y, Zheng W, Pant BD, BlÄSing O, Usadel B, Czechowski T, Udvardi MK, Stitt M, Scheible W-R: **Genome-wide reprogramming of metabolism and regulatory networks of Arabidopsis in response to phosphorus.** *Plant Cell Environ* 2007, **30**:85–112.
11. Muller R, Morant M, Jarmer H, Nilsson L, Nielsen TH: **Genome-wide analysis of the Arabidopsis leaf transcriptome reveals interaction of phosphate and sugar metabolism.** *Plant Physiol* 2007, **143**:156–171.
12. Nilsson L, Muller R, Nielsen TH: **Dissecting the plant transcriptome and the regulatory responses to phosphate deprivation.** *Physiol Plant* 2010, **139**:129–143.
13. Bustos R, Castrillo G, Linhares F, Puga MI, Rubio V, Perez-Perez J, Solano R, Leyva A, Paz-Ares J: **A central regulatory system largely controls transcriptional activation and repression responses to phosphate starvation in Arabidopsis.** *PLoS Genet* 2010, **6**(9). pii: e1001102.
14. Thibaud M, Arrighi J, Bayle V, Chiarenza S, Creff A, Bustos R, Paz-Ares J, Poirier Y, Nussaume L: **Dissection of local and systemic transcriptional responses to phosphate starvation in Arabidopsis.** *Plant J* 2010, **64**(5):775–89.
15. Ji H, Jiang H, Ma W, Johnson DS, Myers RM, Wong WH: **An integrated software system for analyzing ChIP-chip and ChIP-seq data.** *Nat Biotech* 2008, **26**:1293–1300.
16. Saeed AI, Bhagabati NK, Braisted JC, Liang W, Sharov V, Howe EA, Li J, Thiagarajan M, White JA, Quackenbush J: **TM4 microarray software suite.** *Methods Enzymol* 2006, **411**:134–193.
17. Saeed AI, Sharov V, White J, Li J, Liang W, Bhagabati N, Braisted J, Klapa M, Currier T, Thiagarajan M, *et al*: **TM4: a free, open-source system for microarray data management and analysis.** *Biotechniques* 2003, **34**:374–378.
18. Zhang H, Forde BG: **An Arabidopsis MADS Box Gene That Controls Nutrient-Induced Changes in Root Architecture.** *Science* 1998, **279**:407–409.
19. de Folter S, Immink RGH, Kieffer M, Parenicová L, Henz SR, Weigel D, Busscher M, Kooiker M, Colombo L, Kater MM, *et al*: **Comprehensive Interaction Map of the Arabidopsis MADS Box Transcription Factors.** *The Plant Cell Online* 2005, **17**:1424–1433.
20. Zhong R, Lee C, Zhou J, McCarthy RL, Ye Z-H: **A Battery of Transcription Factors Involved in the Regulation of Secondary Cell Wall Biosynthesis in Arabidopsis.** *The Plant Cell Online* 2008, **20**:2763–2782.
21. Zhou J, Lee C, Zhong R, Ye Z-H: **MYB58 and MYB63 Are Transcriptional Activators of the Lignin Biosynthetic Pathway during Secondary Cell Wall Formation in Arabidopsis.** *The Plant Cell Online* 2009, **21**:248–266.
22. Wilson K, Long D, Swinburne J, Coupland G: **A Dissociation Insertion Causes a Semidominant Mutation That Increases Expression of TINY, an Arabidopsis Gene Related to APETALA2.** *The Plant Cell Online* 1996, **8**:659–671.
23. Franco-Zorrilla JM, Martín AC, Leyva A, Paz-Ares J: **Interaction between Phosphate-Starvation, Sugar, and Cytokinin Signaling in Arabidopsis and the Roles of Cytokinin Receptors CRE1/AHK4 and AHK3.** *Plant Physiology* 2005, **138**:847–857.
24. Qin F, Sakuma Y, Tran L-SP, Maruyama K, Kidokoro S, Fujita Y, Fujita M, Umezawa T, Sawano Y, Miyazono K-i, et al: **Arabidopsis DREB2A-Interacting Proteins Function as RING E3 Ligases and Negatively Regulate Plant Drought Stress–Responsive Gene Expression.** *The Plant Cell Online* 2008, **20**:1693–1707.
25. Albrecht V, Ritz O, Linder S, Harter K, Kudla J: **The NAF domain defines a novel protein-protein interaction module conserved in Ca2+–regulated kinases.** *EMBO J* 2001, **20**:1051–1063.
26. Nelson DC, Flematti GR, Riseborough J-A, Ghisalberti EL, Dixon KW, Smith SM: **Karrikins enhance light responses during germination and seedling development in Arabidopsis thaliana.** *Proceedings of the National Academy of Sciences* 2010, **107**:7095–7100.
27. Despres C, DeLong C, Glaze S, Liu E, Fobert PR: **The Arabidopsis NPR1/NIM1 protein enhances the DNA binding activity of a subgroup of the TGA family of bZIP transcription factors.** *Plant Cell* 2000, **12**:279–290.

28. Uno Y, Furihata T, Abe H, Yoshida R, Shinozaki K, Yamaguchi-Shinozaki K: Arabidopsis basic leucine zipper transcription factors involved in an abscisic acid-dependent signal transduction pathway under drought and high-salinity conditions. *Proc Natl Acad Sci U S A* 2000, **97**:11632–11637.

29. Zhang L-Y, Bai M-Y, Wu J, Zhu J-Y, Wang H, Zhang Z, Wang W, Sun Y, Zhao J, Sun X, *et al*: Antagonistic HLH/bHLH Transcription Factors Mediate Brassinosteroid Regulation of Cell Elongation and Plant Development in Rice and Arabidopsis. *The Plant Cell Online* 2009, **21**:3767–3780.

30. Pandey SP, Somssich IE: The Role of WRKY Transcription Factors in Plant Immunity. *Plant Physiology* 2009, **150**:1648–1655.

31. Jung K-H, Seo Y-S, Walia H, Cao P, Fukao T, Canlas PE, Amonpant F, Bailey-Serres J, Ronald PC: The Submergence Tolerance Regulator Sub1A Mediates Stress-Responsive Expression of AP2/ERF Transcription Factors. *Plant Physiology* 2010, **152**:1674–1692.

32. Yang C-Y, Hsu F-C, Li J-P, Wang N-N, Shih M-C: The AP2/ERF Transcription Factor AtERF73/HRE1 Modulates Ethylene Responses during Hypoxia in Arabidopsis. *Plant Physiology* 2011, **156**:202–212.

33. Ascencio-Ibáñez JT, Sozzani R, Lee T-J, Chu T-M, Wolfinger RD, Cella R, Hanley-Bowdoin L: Global Analysis of Arabidopsis Gene Expression Uncovers a Complex Array of Changes Impacting Pathogen Response and Cell Cycle during Geminivirus Infection. *Plant Physiology* 2008, **148**:436–454.

34. Wang Y, Zhang W-Z, Song L-F, Zou J-J, Su Z, Wu W-H: Transcriptome Analyses Show Changes in Gene Expression to Accompany Pollen Germination and Tube Growth in Arabidopsis. *Plant Physiology* 2008, **148**:1201–1211.

35. Oono Y, Seki M, Satou M, Iida K, Akiyama K, Sakurai T, Fujita M, Yamaguchi-Shinozaki K, Shinozaki K: Monitoring expression profiles of <i>Arabidopsis genes during cold acclimation and deacclimation using DNA microarrays. *Functional & Integrative Genomics* 2006, **6**:212–234.

36. Hanada K, Sawada Y, Kuromori T, Klausnitzer R, Saito K, Toyoda T, Shinozaki K, Li W-H, Hirai MY: Functional Compensation of Primary and Secondary Metabolites by Duplicate Genes in Arabidopsis thaliana. *Molecular Biology and Evolution* 2011, **28**:377–382.

37. Lee J-Y, Colinas J, Wang JY, Mace D, Ohler U, Benfey PN: Transcriptional and posttranscriptional regulation of transcription factor expression in Arabidopsis roots. *Proceedings of the National Academy of Sciences* 2006, **103**:6055–6060.

38. Osuna D, Usadel B, Morcuende R, Gibon Y, Bläsing OE, Höhne M, Günter M, Kamlage B, Trethewey R, Scheible W-R, Stitt M: Temporal responses of transcripts, enzyme activities and metabolites after adding sucrose to carbon-deprived Arabidopsis seedlings. *The Plant Journal* 2007, **49**:463–491.

39. Ramel F, Sulmon C, Cabello-Hurtado F, Taconnat L, Martin-Magniette M-L, Renou J-P, El Amrani A, Couee I, Gouesbet G: Genome-wide interacting effects of sucrose and herbicide-mediated stress in Arabidopsis thaliana: novel insights into atrazine toxicity and sucrose-induced tolerance. *BMC Genomics* 2007, **8**:450.

40. Journot-Catalino N, Somssich IE, Roby D, Kroj T: The Transcription Factors WRKY11 and WRKY17 Act as Negative Regulators of Basal Resistance in Arabidopsis thaliana. *The Plant Cell Online* 2006, **18**:3289–3302.

41. Rubio V, Linhares F, Solano R, Martin AC, Iglesias J, Leyva A, Paz-Ares J: A conserved MYB transcription factor involved in phosphate starvation signaling both in vascular plants and unicellular algae. *Genes Dev* 2001, **15**(16):2122–33.

42. Franco-Zorrilla JM, Valli A, Todesco M, Mateos I, Puga MI, Rubio-Somoza I, Leyva A, Weigel D, Garcia JA, Paz-Ares J: Target mimicry provides a new mechanism for regulation of microRNA activity. *Nat Genet* 2007, **39**(8):1033–7.

43. Cheng Y, Zhou W, El Sheery NI, Peters C, Li M, Wang X, Huang J: Characterization of the Arabidopsis glycerophosphodiester phosphodiesterase (GDPD) family reveals a role of the plastid-localized AtGDPD1 in maintaining cellular phosphate homeostasis under phosphate starvation. *Plant J* 2011, **66**(5):781–95.

44. Essigmann B, Guler S, Narang RA, Linke D, Benning C: Phosphate availability affects the thylakoid lipid composition and the expression of SQD1, a gene required for sulfolipid biosynthesis in Arabidopsis thaliana. *PNAS* 1998, **95**(4):1950–5.

45. Cruz-Rumirez A, Oropeza-Aburto A, Razo-Hernandez F, Ramirez-Chavez E, Herrera-Estrella L: Phospholipase DZ2 plays an important role in extraplastidic galactolipid biosynthesis and phosphate recycling in Arabidopsis roots. *Genes Dev* 2006, **103**(17):6765–70.

46. Williamson LC, Ribrioux SP, Fitter AH, Leyser HM: Phosphate availability regulates root system architecture in Arabidopsis. *Plant Physiol* 2001, **126**(2):875–82.

47. Tominaga R, Iwata M, Sano R, Inoue K, Okada K, Wada T: Arabidopsis CAPRICE-LIKE MYB 3 (CPL3) controls endoreduplication and flowering development in addition to trichome and root hair formation. *Development* 2008, **135**(7):1335–45.

48. Lelandais-Brière C, Jovanovic M, Torres GAM, Perrin Y, Lemoine R, Corre-Menguy F, Hartmann C: Disruption of AtOCT1, an organic cation transporter gene, affects root development and carnitine-related responses in Arabidopsis. *The Plant Journal* 2007, **51**:154–164.

49. Bari R, Datt Pant B, Stitt M, Scheible W-R: PHO2, MicroRNA399, and PHR1 Define a Phosphate-Signaling Pathway in Plants. *Plant Physiology* 2006, **141**:988–999.

50. Rouached H, Arpat A, Poirier Y: Regulation of phosphate starvation responses in plants: signaling players and cross-talks. *Mol Plant* 2010, **3**(2):288–99.

51. Dello Ioio R, Linhares FS, Scacchi E, Casamitjana-Martinez E, Heidstra R, Costantino P, Sabatini S: Cytokinins Determine Arabidopsis Root-Meristem Size by Controlling Cell Differentiation. *Current Biology* 2007, **17**:678–682.

52. Okushima Y, Fukaki H, Onoda M, Theologis A, Tasaka M: ARF7 and ARF19 regulate lateral root formation via direct activation of LBD/ASL genes in Arabidopsis. *Plant Cell* 2007, **19**:118–130.